Lateral-torsional-roll response of long precast concrete girders: Uncracked buckling load

William D. Galik, Richard Wiebe, John F. Stanton

- Lateral buckling of precast and prestressed concrete girders that are not fully restrained against twisting rotations at their ends may occur during lifting and handling.
- Typically, the critical load at which this instability occurs has been estimated by ignoring torsional deformations, which is unconservative.
- This study develops a series solution to include torsional deformations for the simplest case of an end-supported girder. The single-term truncation of the series solution provides a nearly exact solution form that permits analysis of practical scenarios, such as girders with camber and overhangs.

All girders are subject to potential lateral-torsional deformations, in which vertical load can cause the girder to bend laterally and rotate about its longitudinal axis. Those deformations may lead to instability. In steel construction, the phenomenon is most prevalent for girders in their final position, at which time they are loaded with full dead and live load but are prevented from rotating at their ends. This buckling mode involves lateral deflections and torsional rotations and is called lateral-torsional buckling. During handling of steel girders, the self-weight alone is generally too light to cause lateral-torsional buckling. For prestressed concrete bridge girders, on the contrary, lateral stability problems are most often associated with handling conditions. Such girders are typically stiffer in torsion and heavier than their steel counterparts. The high torsional stiffness means that lateral instability is unlikely to occur in service, when the ends are twist-restrained, despite the load being its highest. However, during trucking and lifting (**Fig. 1**), the girder is not fully restrained against roll and it may therefore buckle by bending laterally and undergoing rigid-body roll about the longitudinal axis. This instability mechanism is often called roll buckling, but it is termed lateral-roll buckling in this article to explicitly denote the deformation components assumed to be engaged in the buckling mechanism. It is important to distinguish between twist, which involves deformation of the girder, and roll, which is a rigid-body rotational displacement. Instability due to lateral-roll buckling becomes more likely as slenderness increases.

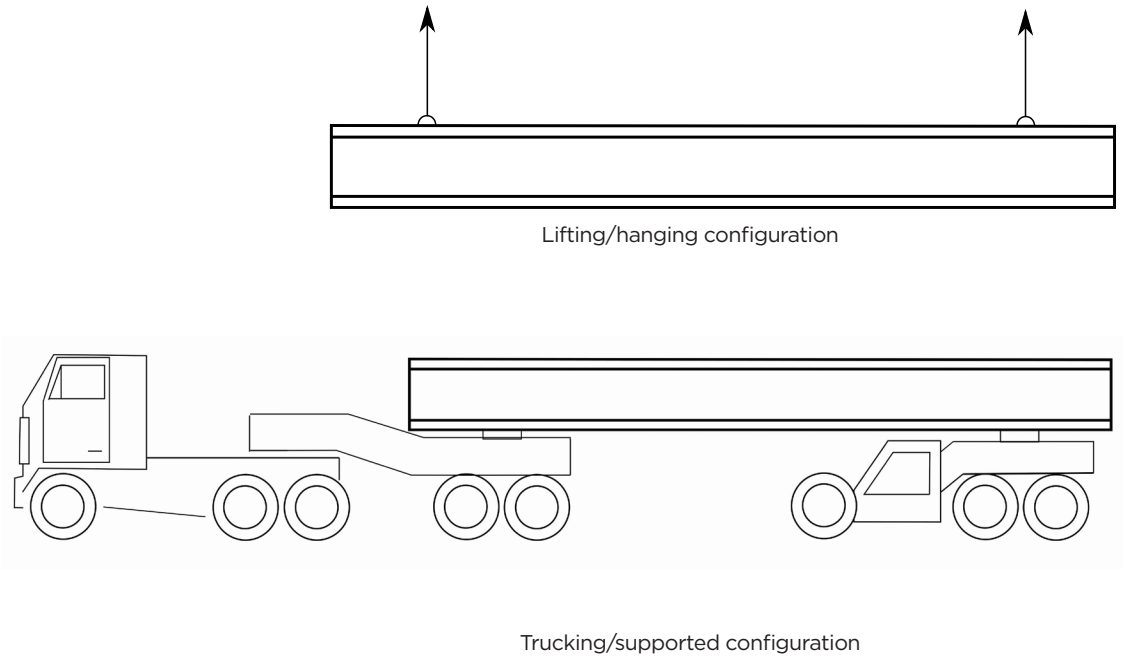

Figure 1. Schematics of conditions for which the girder may roll.

In recent decades, the use of prestressed concrete girders has become increasingly widespread because they are initially cost-effective and need little maintenance during their lifetime. However, span lengths have been increasing as the placement of intermediate piers has become challenging due to both environmental considerations and urban congestion.

The recent placement of a 223 ft (68.0 m) long precast concrete girder in Washington state[1] highlights a trend of lateral stability issues as longer, more slender concrete girders are constructed. The Washington girder was constructed with a WF100TDG cross section (where WF designates wide flange, 100 represents the girder depth in inches and TDG signifies thin deck girder) that was modified from the standard Washington State Department of Transportation (WSDOT) WF100G (**Fig. 2**)[2] by increasing the top flange width by 12 in. (300 mm) to improve the weak-axis moment of inertia and hence the stability of the long girder. Despite the modifications, excessive lateral deflections and relative twist were observed during placement, so the girders were straightened and intermediate lateral bracing was installed before further work was undertaken. The identification of torsional deformations, which are largely ignored in design procedures, raised concerns about the role of torsion in precast concrete girder instability. Oesterle et al.,[3] Rose,[4] and Zureick[5] provide other reports of precast concrete girder stability issues.

Motivated by the observations from the Washington project and general concerns about increasing spans, the work herein re-evaluates current procedures for estimating stability of long precast concrete girders. An important consideration is the relative role of the different deformation components on girder stability. The three important types of deformations that may occur are as follows:

- minor-axis deflection
- rigid-body rotation (roll) about the longitudinal axis
- torsional deformations (twist) about the longitudinal axis

In common cases of instability, at least two of these deformation types are coupled. During handling, the roll and lateral deflection nominally represent the least stiff, and therefore the dominant, modes of deformation. The pioneering analysis by Mast[6] leveraged this fact to provide elegantly simple stability equations that neglect twist deformation and major-axis bending. Mast's assumption that the torsional deformations are small simplifies the analysis while still providing adequate stability estimates for girders of lengths used in the past. Current design procedures[7,8] are based on Mast's work and neglect twist deformation. However, ignoring any source of deformation produces unconservative stability estimates. When torsional flexibility (**Fig. 3**) is accounted for, the critical condition is labeled lateral-torsional-roll buckling because all three deformations (lateral bending, torsional deformation, and rigid-body roll) are involved in the instability mechanism. This article demonstrates that, when roll is possible, ignoring twist flexibility becomes increasingly unconservative with increasing slenderness.

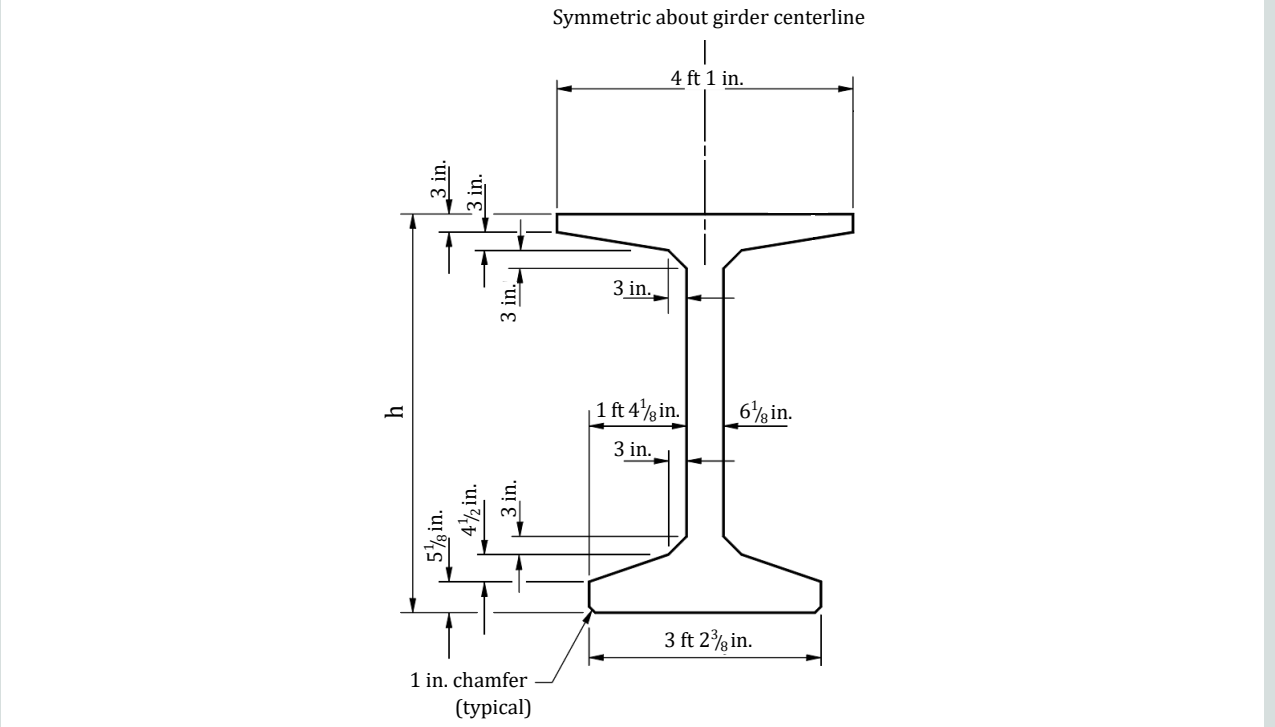

Figure 2. Standard details of Washington State Department of Transportation (WSDOT) WF-series girder. Note: 1 in. = 25.4 mm; 1 ft = 0.305 m. Source: Adapted from WSDOT (2020).

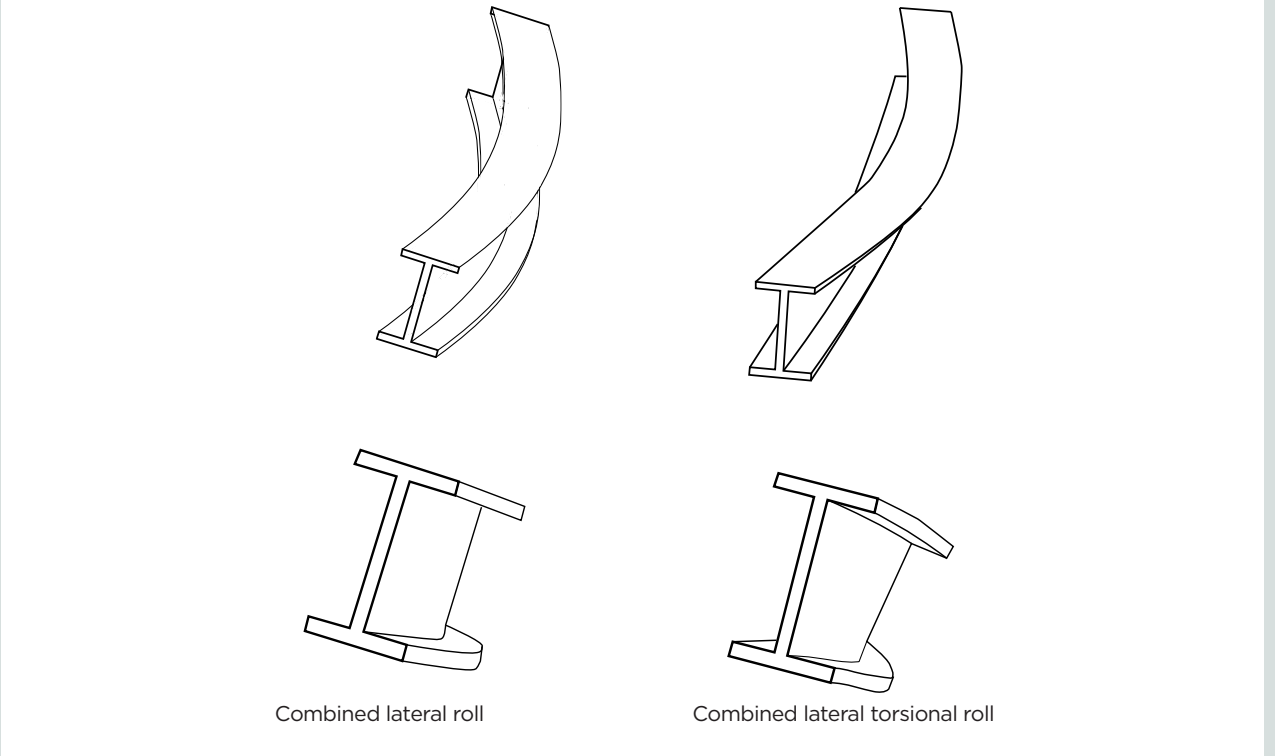

Figure 3. Deflection schematics.

Objectives and scope

The work reported herein forms part of a broader study. This part addresses the effect of torsional deformations and major-axis deflections on the elastic buckling load of uncracked girders as a function of the span, support conditions, and cross-sectional properties. The elastic buckling load of a perfect structural element is not necessarily a failure condition because the behavior of real members is complicated by geometric imperfections and inelastic behavior. It is more important to find the largest deformations that could be accommodated without the prior occurrence of some undesirable behavior, such as cracking or inelastic collapse. Further work, now ongoing, focuses on building a numerical tool to capture the effects of concrete cracking and symmetry-breaking imperfections (such as sweep, wind, or lifting loop eccentricity) on deflection amplification. As a necessary step, the present analytical study develops a closed-form solution to the lateral-torsional-roll buckling problem. The long-term goal is to develop design procedures based on the parameter groupings from the closed-form solution that are adjusted by coefficients produced during the ongoing numerical work.

The scope of this paper includes the following:

- a review of the present methods (primarily based on the pioneering work of Mast) for calculation of buckling loads (lateral-roll buckling) of long-span girders
- a unification of the treatment of hanging and truck-supported configurations (Fig. 1)
- an extension of Mast's approach to include the following practical scenarios:
  - effects of major-axis deflections
  - prestress-induced upward displacement (camber)
  - asymmetric overhangs
- the development of a closed-form equation for the lateral-torsional-roll buckling load in the simplest case of an end-supported girder for which the centroid and shear center are nearly coincident (the solution is in the form of a series solution)
- the extension of the closed-form lateral-torsional-roll buckling formulation to include the already listed practical scenarios

Previous research on buckling load of concrete girders

For concrete components, some of the earliest investigations of what is herein termed lateral-torsional-roll buckling were those of Lebelle[9] and Swann and Godden.[10] Both of those studies included torsional deformations but did not result in a simple equation suitable for design because they used numerical methods. Thus, the findings from those investigations have not been widely used. Furthermore, the prestressed concrete girders of the time were short enough that lateral stability was seldom a problem.

The level of concern about lateral stability changed in 1971 when Anderson[11] reported incipient girder instability when a girder was lifted from the casting bed. That report was a precursor to work by Mast,[6,12] who greatly simplified the analysis by ignoring torsional deformations. He provided an approximate analysis to show that the torsionally rigid assumption was justified for the girders of that era. That work has formed the basis for much of PCI's published information on lateral stability.[7,13]

Stratford and Burgoyne[14] used nonlinear finite element analysis, including torsional flexibility and warping, to evaluate buckling loads. They presented the results in the form of dimensionless design charts. The usefulness of those charts in the present context is questionable because the longest beam commercially available to them at the time in 1999 was 132 ft (40 m), which colors Stratford and Burogyne's finding that torsional deformations could reasonably be ignored. Moreover, the beams analyzed (SY beams used in the United Kingdom) had cross sections different from those used today in the United States. Those beams consisted of narrow bottom flanges, no top flange (to save weight) and thick webs. Therefore, they had a relatively low ratio of minor axis-bending stiffness EI_{yy} (where E is the modulus of elasticity and I_{yy} is the minor-axis second moment of area) to torsional stiffness GJ (where G is the shear modulus and J is the second polar moment of area). Stratford and Burgoyne investigated three conditions:

- simply supported on supports from below that prevented end rotations about the longitudinal axis (herein termed z-rotation)
- transportation by truck with infinitely rigid suspension, but a roller at the rear trailer that allowed free z-rotation at that end
- hanging from yoked, inclined cables

They found that hanging was the most critical condition. The trucks in the United Kingdom that they considered were about an order of magnitude stiffer against roll than the trucks mentioned by Mast. Stratford and Burgoyne[15] subsequently simplified the analysis for the purportedly critical hanging condition by ignoring the torsional deformations. Stratford, Burgoyne, and Taylor[16] presented design equations based on the lateral-roll buckling (that is, no torsion) simplification, which simplify to the expressions proposed by Mast[6] for the case of vertical lifting cables.

Later, Cojocaru[17] and Plaut and Moen[18] included torsion but based their analyses on a doubly symmetric, curved beam.

The resulting equations are not user-friendly as a basis for simplified design equations and result in a singularity if the radius of curvature of the beam is infinite (that is, if the beam is straight). This is a disadvantage in the present circumstances.

The effect of overhangs has been investigated by several researchers. Mast,[6] Peart et al.,[19] and Stratford and Burgoyne[14] all found that bringing in the lifting points from the girder ends greatly increased the buckling load. However, all authors assumed equal overhangs at each end, whereas trucking configurations for contemporary long girders often necessitate unequal overhangs. In review of the literature, no work was found that considered unequal overhangs.

The effects of major-axis deflection and camber have been studied by a few authors. Pi and Trahair[20] and Trahair and Woolcock[21] showed that when neither EI_{yy} nor GJ is negligibly small compared with major-axis flexural rigidity EI_{xx} (where I_{xx} is the major-axis second moment of area), the buckling load is increased due to prebuckling self-weight deflection. Peart et al.[19] used an infinite series solution (and included torsion) to show that the opposite was true for hanging components with net upward camber, such as usually occurs in prestressed concrete girders. For the special case of girders with twist restraint at their ends (that is, classical lateral-torsional buckling) and negligible warping, Peart et al. suggested that camber has no practical effect on the buckling load.

The separation between the shear center and centroid was mentioned by Stratford and Burgoyne[14] and Cojocaru[17] as a parameter that affects the response of lifted beams. Neither author explained the significance of this parameter, nor did they provide equations to illustrate its effect. The effect has been explored for lateral-torsional buckling of monosymmetric sections, where it has been shown[22] that the buckling load can be calculated via an effective GJ that increases with the relative contribution of the beam's compression flange to the weak-axis moment of inertia. Because traditional precast concrete sections in the United States are nearly doubly symmetric, this paper foregoes the consideration of monosymmetry effects, although that factor should potentially be considered in future work.

Lateral-roll buckling

The exact uniformly distributed line load that causes lateral-roll buckling q_{LRB} is approximated in this section for several levels of refinement. When appropriate, the level of refinement is explicitly denoted with additional subscripts. For example, $q_{LRB,0}$ is the classical lateral-roll buckling load by Mast, whereas $q_{LRB,vp\alpha}$ is the lateral-roll buckling load of a girder with asymmetric overhangs (subscript α) and major-axis deflections due to gravity (subscript v) and prestressing (subscript p). Throughout this work, consideration of these practical scenarios (subscripts v, p, α) is referred to as increasing the fidelity level of the buckling load approximation. A higher-fidelity approximation accounts for more of the influential parameters, indicated by the subscripts, and so relies on fewer assumptions.

Coordinate system

The chosen coordinate system **(Fig. 4)** consists of two right-handed coordinate sets: a fixed global coordinate set $(x_{glo},y_{glo},z_{glo})$ that remains oriented with the undeformed beam and a local coordinate set $(x_{loc},y_{loc},z_{loc})$ that travels with the cross section as it displaces. Associated displacements are $(u_{glo},v_{glo},w_{glo})$ and $(u_{loc},v_{loc},w_{loc})$ for the global and local coordinate sets, respectively. The origin is placed at the center of gravity of the concrete of the cross section. For the nearly doubly symmetric beam sections considered in this work, the center of gravity of the concrete practically aligns with the shear center. Coordinate directions are defined such that y_{glo} is vertical and positive downward (meaning self-weight is positive), while rotation about the z_{glo} axis θ is positive clockwise as the z_{glo} axis is oriented into the page.

Treatment of boundary conditions

Most investigators have separately considered the two cases (Fig. 1), which represent a hanging girder and a girder supported from below by a rotationally flexible bearing or truck. However, for analysis of the uncracked condition, the material

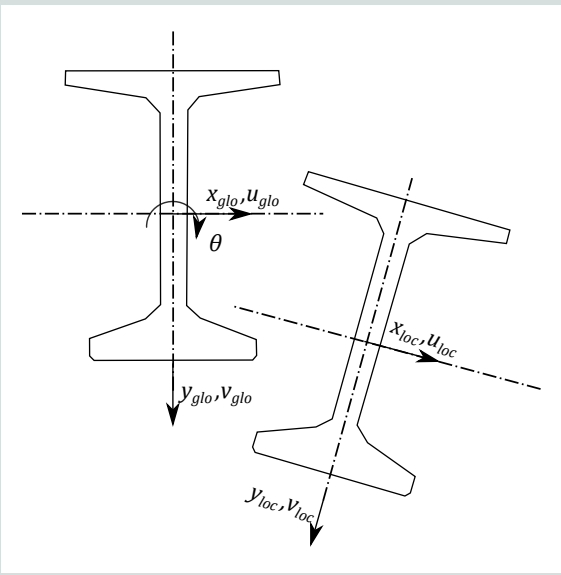

Figure 4. Coordinate systems, with positive sense of rotation and deflections shown. Note: u_{glo} = x displacement component in the global reference frame; u_{loc} = x displacement component in the local reference frame; v_{glo} = y displacement component in the global reference frame; v_{loc} = y displacement component in the local reference frame; x_{glo} = x position coordinate in the global reference frame; x_{loc} = x position coordinate in the local reference frame; y_{glo} = y position coordinate in the global reference frame; y_{loc} = y position coordinate in the local reference frame; z_{loc} = z position coordinate in the local reference frame; θ = girder rotation about longitudinal z axis.

models are linear, and both cases can be modeled as having a total rotational stiffness located at the center of gravity due to stiffness at supports and lifting loops K_θ. **Figure 5** (cross section at one support of a symmetric girder) shows that the external restoring torque T is calculated by Eq. (1).

$$T = -Ry_r \sin\theta + K_{\theta,sup}\theta \quad (1)$$

where

R = vertical reaction at girder support (positive downward, in other words, it typically takes negative values)

y_r = vertical distance from the center of gravity of concrete to the support point (positive downward)

$K_{\theta,\text{sup}}$ = support rotational stiffness due to rotational bearing or truck stiffness (equal to zero for a hanging girder)

For girders without imperfections (as in this study), small rotations can be assumed for loads below the buckling load so that the moment equilibrium equation can be simplified to Eq. (2).

$$T = -(Ry_r - K_{\theta,sup})\theta \quad (2)$$

Equation (3) defines the term in parentheses as the total rotational stiffness K_θ.

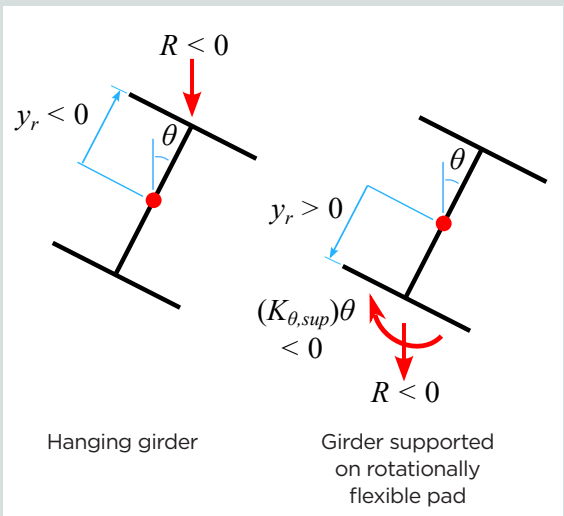

Figure 5. Torsional restoring moment. Note: Arrows are drawn according to positive sign convention, with negative support reactions noted accordingly. $K_{\theta,sup}$ = support rotational stiffness due to rotational bearing or truck stiffness; R = shear reaction at girder support (positive downward); y_r = vertical (hanging) distance from the center of gravity of concrete to the support point; z_{loc} = z position coordinate in the local reference frame; θ = girder rotation about longitudinal z axis.

$$K_\theta = Ry_r - K_{\theta,sup} \quad (3)$$

The same moment equilibrium equation can be used regardless of the support conditions, provided that an appropriate value is assigned to K_θ. This work focuses on the hanging girder case, but the same analysis is valid for the supported girder by defining an equivalent hanging distance $y_{r,eq}$, that is valid for both a hanging girder or a girder supported from below (Eq. [4]).

$$y_{r,eq} = \frac{K_\theta}{R} = y_r - \frac{K_{\theta,\text{sup}}}{R} \quad (4)$$

In Eq. (4), y_r is positive for a girder supported from below because vertical distance is taken as positive downward. The restoring torque is written in general form as Eq. (5).

$$T = -Ry_{r,eq}\theta \quad (5)$$

The equivalent hanging distance $y_{r,eq}$ will be used throughout the remainder of the paper.

Equilibrium configuration of an imperfect system

Mast[6] evaluated lateral-roll buckling of hanging girders by considering the equilibrium of a girder with an eccentric lifting loop placement e_x. **Figure 6** shows the geometry of the system in its displaced configuration, where the full girder weight W is collinear with the lifting loop position. The initial eccentricity is used here simply as a tool for determining the buckling load. A study of the effects of imperfections of different types is beyond the scope of this work.

A component of the girder's self-weight acts in the x_{loc} direction, so the girder bends laterally and the center of gravity of the concrete of the entire girder is displaced. It is useful to introduce the displacement of a prismatic simply supported beam subject to a distributed load.

$$\Delta(\zeta) = \frac{qL^4}{EI}\left(\frac{\zeta^4 - 2\zeta^3 + \zeta}{24}\right) \quad (6)$$

where

Δ = displacement of a prismatic simply supported beam subjected to a distributed load

ζ = normalized measure of distance along girder length = z/L

z = measure of distance along girder length

L = total girder length

q = distributed load on girder (positive downward)

E = modulus of elasticity

I = second moment of area

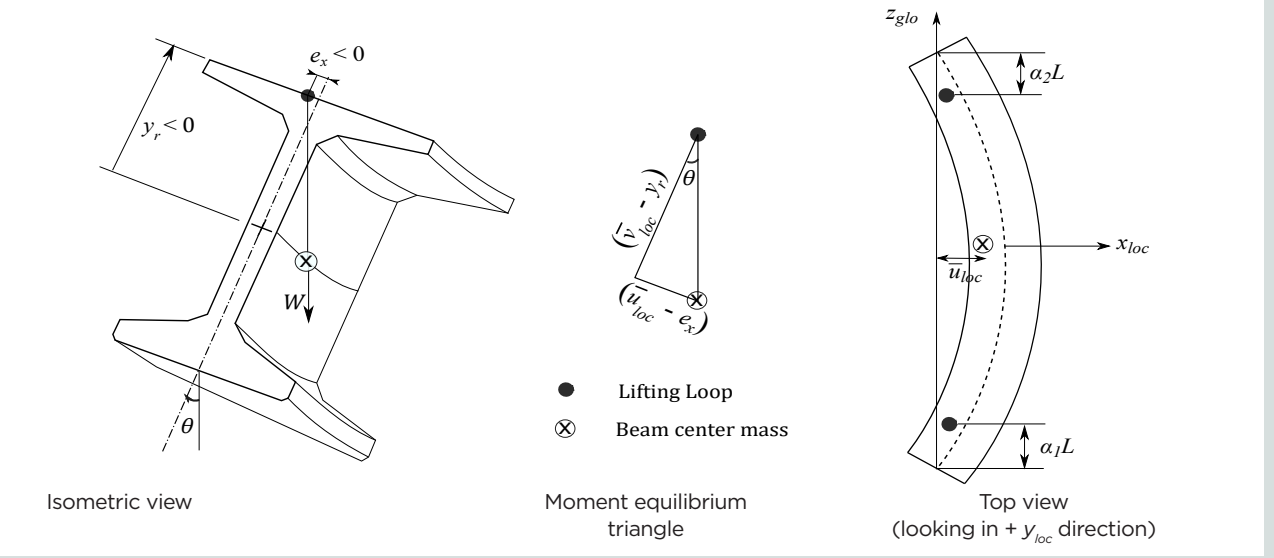

Figure 6. Lateral-roll deformation of a beam with a positive roll angle due to a negative lifting-loop eccentricity. Note: e_x = lifting loop eccentricity (positive in +x direction); L = total girder length; u_{loc} = x displacement component in the local reference frame; $\bar{u}_{loc}$ = x displacement component of girder center of mass; v_{loc} = y displacement component in the local reference frame; W = total girder weight; y_r = vertical (hanging) distance from the center of gravity of concrete to the support point; z_{glo} = z position coordinate in the global reference frame; z_{loc} = z position coordinate in the local reference frame; α_1 = overhang ratio at end 1; α_2 = overhang ratio at end 2; θ = girder rotation about longitudinal z axis.

Taking the average over the span of Eq. (6) results in a coefficient of 1/120 for the case of no overhangs. The average beam deflections in the x_{loc} and y_{loc} directions due to a unit distributed load are specialized as the compliance coefficients (where overbars are used to indicate average values) calculated in Eq. (7) and (8).

$$\bar{c}_x = \frac{L^4}{120EI_{yy}} \tag{7}$$

where

$\bar{c}_x$ = compliance coefficient for minor-axis deflection

$$\bar{c}_y = \frac{L^4}{120EI_{xx}} \tag{8}$$

where

$\bar{c}_y$ = compliance coefficient for major-axis deflection

The applied distributed load q acts downward and is positive. For the rotated beam, the load magnitudes acting in the x_{loc} and y_{loc} directions are $q(\sin\theta)$ and $q(\cos\theta)$, respectively. While the load of interest for these problems is typically the self-weight, the equations are developed for a distributed load of arbitrary magnitude. Equations (9) and (10) calculate the center-of-mass displacements in the x_{loc} and y_{loc} directions, respectively, of a torsionally rigid, end-supported girder subjected to a uniform distributed line load, in the absence of camber.

$$\bar{u}_{loc} = \bar{c}_x q \sin\theta = \frac{qL^4}{120EI_{yy}} \sin\theta \tag{9}$$

where

$\bar{u}_{loc}$ = center-of-mass displacement in x_{loc} direction of a torsionally rigid, end-supported girder subjected to a uniform distributed line load in the absence of camber

$$\bar{v}_{loc,v} = \bar{c}_y q \cos\theta = \frac{qL^4}{120EI_{xx}} \cos\theta \tag{10}$$

where

$\bar{v}_{loc,v}$ = center-of-mass displacement in y_{loc} direction of a torsionally rigid, end-supported girder subject to uniform distributed line load in the absence of camber

The subscript v is included in Eq. (10) to distinguish the vertical deflection due to applied loads from the vertical deflections due to internal cambering loads. (This distinction is discussed later.)

Equations (9) and (10) include three unknowns: the two coordinates of the center of mass of the girder, and the roll angle. The system is solved by enforcing moment equilibrium as a third equation, which is satisfied when the self-weight and lifting loop reactions are collinear. This is done at several different levels of fidelity in the following sections.

Development of Mast's critical load

Mast[6] ignored the component of major-axis deflection and

obtained Eq. (11), a collinearity equation (Fig. 6 with $\overline{v}_{loc,v}$ equal to 0 and $y_{r,eq}$ less than 0).

$$-y_{r,eq}\tan\theta = \overline{u}_{loc} - e_x \tag{11}$$

This equation allows the girder rotation about the longitudinal axis θ to be computed for a known section and given lifting loop eccentricity in the absence of twist deformations. Because the girder rotates as a rigid body, this displacement is colloquially called roll. In the equation, θ is not limited to being small.

The initial girder roll angle due to eccentric lifting-loop support θ_i may be defined as the rigid-body roll angle for a girder that has initial imperfections but is undeformed by the loads. An expression for the initial roll angle is provided in Eq. (12).

$$\tan\theta = \frac{e_x}{y_{r,eq}} \tag{12}$$

Combining Eq. (9), (11), and (12) and rearranging gives Eq. (13).

$$\tan\theta = \frac{\tan\theta_i}{1 + \dfrac{q}{y_{r,eq}/\overline{c}_x}\cos\theta} \tag{13}$$

If θ is taken to be small, cos θ equals 1.0 and Eq. (13) takes the form of a magnification factor, similar to the one often used for column buckling. Any initial roll angle becomes magnified without bound when q approaches $-y_{r,eq}/\overline{c}_x$. It follows that Eq. (14) defines the lateral-roll buckling load derived by Mast[6] $q_{LRB,0}$.

$$q_{LRB,0} = -\frac{y_{r,eq}}{\overline{c}_x} = -\frac{120EI_{yy}y_{r,eq}}{L^4} \tag{14}$$

The presence of the average compliance coefficient in Eq. (14) indicates that only the net displacement of the center of mass is relevant for calculating the lateral-roll buckling load (for prismatic girders).

Incorporation of downward major-axis deflection

This section extends the results of Mast's work[6] to include downward major-axis deformation. Figure 6 shows the deformed girder configuration when major-axis gravity deflections are included. Again, applying the collinearity assumption yields Eq. (15).

$$(\overline{v}_{loc,v} - y_{r,eq})\tan\theta = \overline{u}_{loc} - e_x \tag{15}$$

Substituting the average deflections in the local reference frame (Eq. [9] and [10]) and rearranging gives Eq. (16).

$$-y_{r,eq}\tan\theta = \overline{u}_{loc}\left(1 - \frac{I_{yy}}{I_{xx}}\right) - e_x \tag{16}$$

This expression is identical to Eq. (11) except for the added factor of $(1 - I_{yy}/I_{xx})$.

Again, following the procedure of Mast[6] (that is, buckling-load-by-magnification) produces Eq. (17), which defines the lateral-roll buckling load of a girder with major-axis deflections due to gravity.

$$q_{LRB,v} = -\frac{120EI_{yy}y_{r,eq}}{L^4\left(1 - \dfrac{I_{yy}}{I_{xx}}\right)} = q_{LRB,0}\frac{1}{1 - \dfrac{I_{yy}}{I_{xx}}} \tag{17}$$

The subscript v indicates that this result incorporates strong-axis deflection. As the ratio I_{yy}/I_{xx} increases, the critical load increases. This agrees with the findings of Trahair and Woolcock.[21] When I_{yy}/I_{xx} is greater than or equal to 1.0, the buckling load transitions through a pole from positive to negative infinity, implying that buckling is impossible. This unconditional stability is reflected in the fact that the American Institute of Steel Construction's *Specification for Structural Steel Buildings* (AISC 360)[23] allows, without giving reasons, lateral buckling to be ignored for a steel beam bent about its minor axis. A double tee is an example of a member with I_{yy}/I_{xx} greater than or equal to 1.0. It is inherently stable during lifting.

Figure 7, which plots Eq. (17) normalized by $q_{LRB,0}$, illustrates the effect of major-axis deformation on the lateral-roll buckling load. For prestressed concrete bridge girders, the value of I_{yy}/I_{xx} varies among different section shapes but is generally less than about 0.25. The specific values for several example shapes are shown in the figure for illustration, where gravity deflections have a stabilizing effect (in the absence of camber). Upward camber produces an offsetting destabilizing effect, as will be discussed in the next section.

Incorporation of draped prestressing effects

Long prestressed concrete girders will typically display a net upward camber under the combined effects of prestress and self-weight. For the analysis of simply supported girders, bottom tendons are herein idealized as being draped parabolically such that they produce an upward deflection equal to what would be caused by an upward uniform load q_p (which is negative-valued because it points upward). Although the true cable layout is not strictly parabolic for a typical pretensioned girder, an equivalent q_p can be calculated for other tendon profiles (for example, straight or harped) without loss of generality. This is done by taking advantage of the net center of mass location observation that accompanied Eq. (14). Thus, an equivalent uniform q_p can always be obtained, provided that it produces an average deflection that is the same as that caused by the actual strand pattern.

Note that the nominal prestressing load q_p remains oriented with the major axis as the girder rotates. For reference, girders long enough to require stability analysis typically have the following condition:

$$-2.5 \le \frac{q_p}{q_{sw}} \le -1.5$$

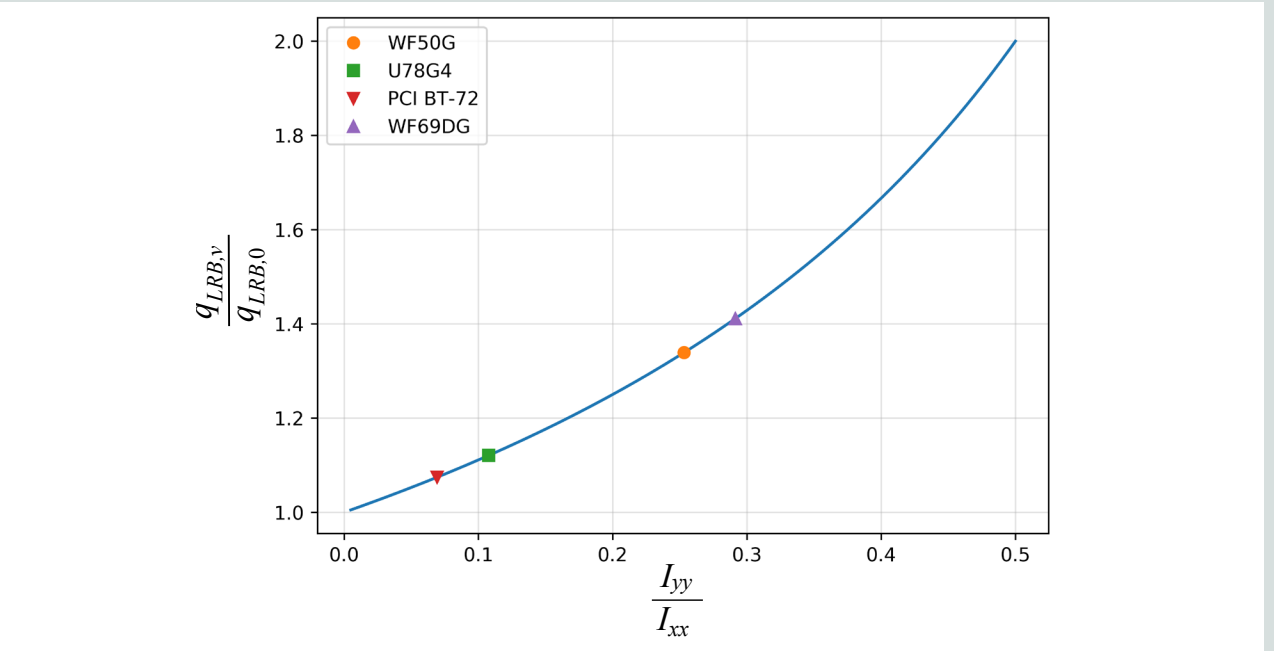

Figure 7. Critical load for girders with flexible major axis, relative to Mast's lateral roll buckling prediction, which assumes the major-axis second moment of area I_{xx} is rigid. The values for four specific girder cross sections are placed on the curve. Note: I_{yy} = minor-axis second moment of area; $q_{LRB,0}$ = classical lateral-roll buckling load derived by Mast; $q_{LRB,v}$ = lateral-roll buckling load of a girder with major-axis deflections due to gravity; U78G4 = tub girder with 84 in. depth and 48 in. soffit width; WF50G = wide-flange girder with 50 in. depth; WF69DG = wide flange deck girder with 69 in. depth; PCIBT-72 = bulb tee with 72 in. depth.

where

q_{sw} = uniformly distributed girder self-weight

In practice, the term *camber* is usually taken to mean net camber, that is, the difference between the deflections due to self-weight (downward) and prestressing (upward). Here, the two loadings cause slightly different deflections when θ does not equal zero because the prestressing remains oriented with the major axis; therefore, the two loadings are treated separately. Considered independently from gravity loads, the nominal prestressing load q_p causes a deflection $v_{loc,p}(z)$ that varies as a function of the longitudinal position. The center of mass displacement in the y_{loc} direction of a torsionally rigid, rotated girder due to the prestressing load, $\overline{v}_{loc,p}$ is calculated using Eq. (18).

$$\overline{v}_{loc,p} = q_p \overline{c}_y \tag{18}$$

In this case, a trigonometric term does not appear because q_p rotates with the girder. Equation (10) can then be generalized to include both the prestressing and gravity effects to produce Eq. (19).

$$\overline{v}_{loc,vp} = \overline{v}_{loc,v} + \overline{v}_{loc,p} = \overline{c}_y \left(q \cos\theta + q_p \right) \tag{19}$$

where

$\overline{v}_{loc,vp}$ = center of mass displacement in y_{loc} direction of a torsionally rigid, end-supported girder due to gravity and prestressing

Again, insertion of the appropriate center-of-mass deflections into the moment equilibrium triangle of Fig. 6 produces an equilibrium expression Eq. (20).

$$-y_{r,eq} \tan\theta = \overline{u}_{loc} \left(1 - \frac{I_{yy}}{I_{xx}} \right) - \overline{v}_{loc,p} \tan\theta - e_x \tag{20}$$

Reorganizing Eq. (20) and solving buckling-load-by-magnification give the lateral-roll buckling load of a girder with major-axis deflections due to gravity and prestressing $q_{LRB,vp}$.

$$q_{LRB,vp} = q_{LRB,0} \frac{\left(1 - \frac{\overline{v}_{loc,p}}{y_{r,eq}} \right)}{\left(1 - \frac{I_{yy}}{I_{xx}} \right)} \tag{21}$$

In Eq. (21), both $\overline{v}_{loc,p}$ and $y_{r,eq}$ are negative, so the effect of upward prestressing is to destabilize the girder and reduce the buckling load.

While Eq. (17) showed that girders without prestressing can avoid buckling unconditionally only if I_{yy}/I_{xx} is greater than or equal to 1.0, this critical ratio increases to the combined conditions $I_{yy}/I_{xx} \geq -q_{LRB,0}/q_p$ and $I_{yy}/I_{xx} \geq 1.0$ when prestressing deflections are included. This phenomenon occurs because when $q + q_p$ is less than 0.0, the girder has a net upward camber and

thus is susceptible to simple inverted pendulum instability even if I_{yy} approaches infinity. In the absence of prestressing, q_p equals 0, and Eq. (20) collapses to Eq. (16). If the magnitudes of the prestressing load q_p and the classical lateral-roll buckling load $q_{LRB,0}$ are equal and opposite, the equilibrium equation (Eq. [20]) can be rearranged to show that the critical girder load matches Mast's classical result. This is because the upright girder immediately prior to the onset of buckling is exactly straight with no major-axis deflection, regardless of I_{yy}/I_{xx}.

Incorporation of overhangs

The equilibrium expression for the simplest scenario without major-axis deflection or camber (Eq. [11]) can be generalized to include the effect of overhangs (which are shown in Fig. 1). The result takes the form of a stabilizing overhang factor that decreases the center-of-mass deflection (thereby increasing the critical load). After the development of the overhang factor for the simple case, the same factor can be used with the more general equations presented in the previous section.

Mast[6] as well as Stratford and Burgoyne[15] have shown that the compliance coefficients in Eq. (7) and (8) are multiplied by a lateral-roll buckling overhang factor for symmetrically supported, torsionally rigid girder $f_{LRB}(\alpha)$, which is less than 1.0.

$$\overline{c}_{x,a} = \frac{L^4}{120EI_{yy}} f_{LRB}(\alpha) \tag{22}$$

where

$\overline{c}_{x,a}$ = compliance coefficient for minor-axis deflection of a beam with overhangs

$$\overline{c}_{y,a} = \frac{L^4}{120EI_{xx}} f_{LRB}(\alpha) \tag{23}$$

where

$\overline{c}_{y,a}$ = compliance coefficient for major-axis deflection of a beam with overhangs

$$f_{LRB}(\alpha) = \sum_{j=0}^{4} b_{LRB,j}\alpha^j \tag{24}$$

α = ratio of overhang distance to total length of girder L

$b_{LRB,j}$ = coefficients for polynomial order j in the lateral-roll buckling overhang factor = [+1, -10, +30, -20, -10]

j = index representing the polynomial degree of α in each term of the overhang factor

Equations (22), (23), and (24) are obtained by evaluating the average deflection, relative to the chord between supports, of a beam with equal overhangs subject to a uniform load. By the same method, the equations are extended here to include unequal overhangs, for which the overhang factor becomes Eq. (25).

$$f_{LRB}(\alpha,t) = \sum_{j=0}^{4} b_{LRB,j}s_j(t)\alpha_m^j \tag{25}$$

where

$f_{LRB}(\alpha,t)$ = overhang factor for an asymmetrically supported, torsionally rigid girder

$s_j(t)$ = fourth-order polynomial in t, representing the effects of asymmetry

t = girder's degree of asymmetry, as a function of the two end-overhang ratios = $(\alpha_1 - \alpha_2)/(\alpha_1 + \alpha_2)$

α_1 = overhang ratio at end 1

α_2 = overhang ratio at end 2

α_m = mean overhang ratio = $(\alpha_1 + \alpha_2)/2$

The overhang coefficients are defined by Eq. (26).

$$s_j(t) = \left[1, 1, \left(1 - \frac{t^2}{3}\right), \left(1 - 3t^2\right), \left(1 - t^2\right)\left(1 + 3t^2\right)\right] \tag{26}$$

The representation of Eq. (25) separates the effect of mean overhang length and asymmetry relative to that mean. The value of t varies from 0.0 (equal overhangs) to 1.0 (no overhang one end). For t equal to 0.0, $f_{LRB}(\alpha,t)$ condenses to the expression in Eq. (24).

When the effects of major-axis deflections and prestressing are included, the lateral-roll buckling condition for a hanging girder with overhangs is solved by substituting Eq. (9), (18), (22), (23), (24), and (25) into Eq. (20). Following the procedure from the earlier section "Development of Mast's Critical Load," it is shown that the beneficial effect of overhangs can be expressed as a stabilization factor. For the load, that expression is Eq. (27).

$$\frac{q_{LRB,vpa}}{q_{LRB,vp}} = \frac{1}{f_{LRB}(\alpha,t)} \tag{27}$$

where

$q_{LRB,vpa}$ = lateral-roll buckling load of a girder with asymmetric overhangs and major-axis deflections due to gravity and prestressing

Figure 8 plots Eq. (27) against the mean overhang value for various degrees of asymmetry. For the symmetric case (t equals 0), the support location that maximizes the overhang factor is 0.23L, which corresponds approximately to the point (0.207L) at which the absolute values of the negative support moment and the peak positive moment are equal. This value represents a shift in behavior, beyond which overhangs trend toward unfavorable cantilever behavior. With unequal overhangs, which may occur in transportation because of trucking vehicle limitations, the peak effectiveness, and the α_m value at which it occurs, reduce as the degree of asymmetry increases.

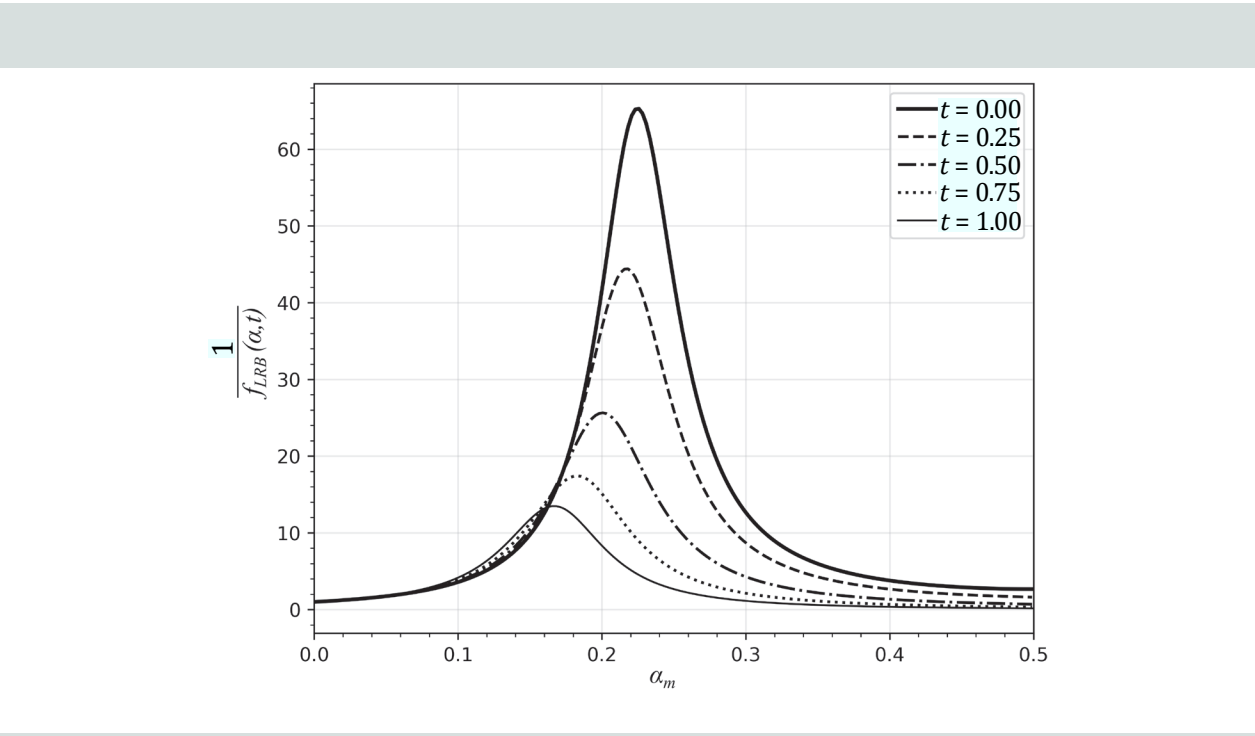

Figure 8. Effect of mean overhang ratio αm and asymmetry factor *t* on lateral-roll stabilization factor. Note: $f_{LRB}(\alpha, t)$ = overhang factor for an asymmetrically supported, torsionally rigid girder.

For completeness, Fig. 8 shows the overhang stabilization factor for the full range of overhangs ($0 \le \alpha_m \le 0.5$). Higher α_m values represent configurations that are impractical for hanging girders, although they may be applicable to other applications, such as spreader beams.[24] Individual overhang values (for example, α_1, α_2) are unlikely to exceed 0.15 to avoid excessive top-flange tension due to prestressing or a large number of top strands. Net top tension reduces the roll angle needed to cause top-flange cracking, which constitutes an important criterion used in safety evaluation of girders. For α_m less than 0.15, the stabilization factor $1/f_{LRB}(\alpha,t)$ is always slightly higher than the stabilization factor for the symmetric case. This allows safe use of the average overhang distance with the simpler Eq. (24) for any realistic prestressed concrete girder, regardless of the asymmetry degree.

If a girder has unequal overhangs, the vertical reaction at each support will be different. If the $y_{r,eq}$ distance is also different at each end, the total resisting torque will be affected, and the buckling load will change. For a prismatic, torsionally rigid, asymmetrically supported girder, the results are the same as for a symmetric girder if the effective hanging distance in Eq. (28) is used.

$$y_{r,eff} = \frac{y_{r1,eq}\left(0.5-\alpha_2\right)+y_{r2,eq}\left(0.5-\alpha_1\right)}{1-\alpha_1-\alpha_2} \quad (28)$$

where

$y_{r,eff}$ = effective hanging distance for asymmetrically supported, torsionally rigid girder with different equivalent hanging distances at each support

$y_{r1,eq}$ = equivalent hanging distance at end 1

$y_{r2,eq}$ = equivalent hanging distance at end 2

Incorporation of torsional deformation

The approach presently used to analyze lateral stability of long precast concrete girders in practice was summarized and extended in the previous section on lateral-roll buckling. That approach relies on the simplifying assumption that girders are stocky enough to be treated as torsionally rigid. These methods are typically derivative of Mast's approach, which decouples the deformation components to find the center of gravity of the concrete. That direct equilibrium approach is more challenging for torsionally flexible girders, so this section instead starts from the governing differential equation for beam twist.

First, a modal approach is used to solve the coupled lateral-torsional-roll buckling problem for the simplest case of a girder hanging from its ends. As is done for the classical lateral-roll buckling[7] and lateral-torsional buckling[25] solutions, the governing equation ignores major-axis flexibility. A one-mode approximation provides insight into a near-exact lateral-torsional-roll buckling solution, in the form of an interaction between lateral-roll buckling and lateral-torsional buckling behavior. Then, the solution form is used to develop a more general lateral-torsional-roll buckling solution that captures major-axis deflections, prestressing, and overhangs. This progression follows the development of the lateral-roll

buckling load described in the previous section for various fidelity levels.

Development of the lateral-torsional-roll buckling design equation

The equation governing the twist angle for an end-supported girder with a uniformly distributed vertical line load, negligible major-axis bending, and no end restraint of warping, written in terms of the unitless variable ζ (equal to z/L) is given by Eq. (29). The appendix provides the derivation.

$$\frac{d^2\theta(\zeta)}{d\zeta^2}+\frac{\kappa^2L^6}{4}\zeta^2(1-\zeta)^2\theta(\zeta)=0 \tag{29}$$

where

$\theta(\zeta)$ = girder rotation about the z axis (twist), along the girder length

κ = load parameter = $q\sqrt{GJEI_{yy}}$

For the classical analysis of lateral-torsional buckling, the boundary conditions are typically twist fully restrained (θ equals 0) or torsionally free ($d\theta/d\zeta$ equals 0). For the lateral-torsional-roll buckling problem, both ends are free to rotate but have a nonzero end torque dictated by the total torsional support stiffness K_θ given in Eq. (3). For the equivalent hanging girder with uniform line load q and no overhangs, the boundary conditions are given in Eq. (30) and (31).

$$M_{z,loc}(\zeta=0)=-\frac{qL}{2}y_{r,eq}\theta_0 \tag{30}$$

where

$M_{z,loc}$ = internal girder moment about the z_{loc} direction

θ_0 = rigid-body roll at supports

$$M_{z,loc}(\zeta=1)=+\frac{qL}{2}y_{r,eq}\theta_0 \tag{31}$$

Using the net-section relationship below in combination with Eq. (30) and (31) gives Eq. (32) and (33).

$$M_{z,loc}=GJ\frac{d\theta}{dz}=\frac{GJ}{L}\frac{d\theta}{d\zeta}.$$

$$\frac{GJ}{L}\frac{d\theta}{d\zeta}\Big|_{\zeta=0}=-\frac{qL}{2}y_{r,eq}\theta(0) \tag{32}$$

$$\frac{GJ}{L}\frac{d\theta}{d\zeta}\Big|_{\zeta=1}=\frac{qL}{2}y_{r,eq}\theta(1) \tag{33}$$

where

$\theta(0)$ = rotation angle at end 1, equal to the rigid-body roll θ_0 if girder is symmetric

$\theta(1)$ = rotation angle at end 2, equal to the rigid-body roll θ_0 if girder is symmetric

The shear center may be separated from the center of gravity of the concrete for a singly symmetric girder. The effect is to alter the torsional rigidity GJ as done, for example, by Anderson and Trahair.[26] For cross sections that are reasonably approximated as doubly symmetric (as in this study), the error in ignoring this effect is small.

To keep the results tractable, a Ritz-Galerkin representation is used for the solution of Eq. (29). This starts from the weak form of the governing equation as illustrated in Eq. (34).

$$\int_0^1\bar{\theta}(\zeta)\left[\frac{d^2\hat{\theta}(\zeta)}{d\zeta^2}+\frac{\kappa^2L^6}{4}\zeta^2(1-\zeta)^2\hat{\theta}(\zeta)\right]d\zeta=0 \tag{34}$$

where

$\bar{\theta}(\zeta)$ = weight function

$\hat{\theta}(\zeta)$ = approximation of the girder twist along the length

The twist approximation function is assumed to have the form of Eq. (35).

$$\hat{\theta}(\zeta)=\theta_0+\sum_{m=1}^{M}\hat{a}_mN_m(\zeta)=\theta_0+[N]\{\hat{a}\} \tag{35}$$

where

M = number of shapes functions employed in the twist approximation

$\hat{a}_m$ = coefficients of the mth twist shape approximation function

$N_m(\zeta)$ = set of twist shape functions that are zero at the girder ends

$[N]$ = twist shape functions collected into a row matrix

$\{\hat{a}\}$ = coefficients of the mth twist shape approximation function collected into a column vector

The function approximation may be refined by increasing the number of shape functions used.

The θ_0 term of Eq. (35) captures the rigid-body roll at the supports, while the scaled shape functions approximate the torsional deformations between supports. Although not done here, this approximation could be extended to allow θ_0 to vary linearly between the two ends. Doing so would extend the solution to cover asymmetric girders but would result in more complex equations. Substituting Eq. (35) into Eq. (32) (equivalently into Eq. [33]) allows for the elimination of θ_0 as a function of the derivative $d\theta/d\zeta$. This yields Eq. (36), a version of the approximate twist function.

$$\hat{\theta}(\zeta)=\frac{-2GJ\dfrac{d\theta(0)}{d\zeta}}{qL^2y_{r,eq}}+[N]\{\hat{a}\}=-\frac{2GJ}{qL^2y_{r,eq}}[B_0]\{\hat{a}\}+[N]\{\hat{a}\} \tag{36}$$

where

$[B_0]$ = derivative of the girder-twist shape function matrix $[N]$ with respect to ζ, evaluated at $\zeta = 0$ (If Eq. [33] were used, this would be evaluated at $\zeta = 1$ but the result would be the same.)

To apply the Galerkin assumption, the weight function in the weak form of the twist-governing equation $\overline{\theta}$ is constructed from the same shape functions as the approximation function, which gives Eq. (37).

$$\overline{\theta}(z) = [N]\{\overline{a}\} = \{\overline{a}\}^T [N]^T \tag{37}$$

where

$\{\overline{a}\}$ = weighting coefficients of the mth weight function, collected into a column vector

Finally, substituting the assumed solution form of Eq. (36) and the weight function from Eq. (37) into Eq. (34) yields Eq. (38), an eigenvalue expression for the buckling load (contained within the parameter κ).

$$\begin{aligned}&\{\overline{a}\}^T \left[\int_0^1 [N]^T \left[\frac{d^2 N}{d\zeta^2} \right] d\zeta \right. \\ &\left. + \frac{\kappa^2 L^6}{4} \int_0^1 \zeta^2 (1-\zeta)^2 [N]^T \left(\frac{-2GJ}{qL^2 y_{r,eq}} [B_0] + [N] \right) d\zeta \right] \{\hat{a}\} \\ &= \{0\}, \forall \{\overline{a}\}\end{aligned} \tag{38}$$

Equation (38) is satisfied for arbitrary values of the weighting coefficients $\{\overline{a}\}$, so the result is a homogeneous system of equations of the form in Eq. (39).

$$[K_{tot}]\{\hat{a}\} = \{0\} \tag{39}$$

where

$[K_{tot}]$ = weak-form coefficient matrix for M-mode approximation of girder twist (bracketed expression in Eq. [38])

Rewriting κ in terms of q from Eq. (29) and collecting the three matrix integrals ($[K_1]$, $[K_2]$, $[K_3]$) from the bracketed term of Eq. (38) gives Eq. (40) to (43).

$$[K_{tot}] = [K_1] - \frac{qL^4}{2EI_{yy} y_{r,eq}} [K_2] + \frac{q^2 L^6}{4GJEI_{yy}} [K_3] \tag{40}$$

where

$$[K_1] = \int_0^1 [N]^T \left[\frac{d^2 N}{d\zeta^2} \right] d\zeta \tag{41}$$

$$[K_2] = \int_0^1 \zeta^2 (1-\zeta)^2 [N]^T [B_0] d\zeta \tag{42}$$

$$[K_3] = \int_0^1 \zeta^2 (1-\zeta)^2 [N]^T [N] d\zeta \tag{43}$$

The critical load can be determined by finding the values of q that produce a singular matrix K_{tot}. In such cases, Eq. (39) would permit arbitrarily large deflections. This defines the buckling load. For the symmetric problem considered herein, the family of odd sine functions provides a basis that captures the exact response (in which case the superscript hat could be removed) in the limit and still produces a good approximation with short truncations. This work leverages a one-mode approximation to avoid computational solutions, which are less tractable for use in design. The one-mode solution leads to a closed-form representation, which allows the relevant dimensionless parameter groupings to be identified. The one-mode shape function N_1 equals sin $\pi\zeta$ and results in a scalar K_{tot} (Eq. [44]).

$$K_{tot} = -k_1 - \frac{k_2 L^4}{EI_{yy} y_{r,eq}} \hat{q}_{LTRB,0} + \frac{k_3 L^6}{GJEI_{yy}} \hat{q}_{LTRB,0}^2 = 0 \tag{44}$$

where the bracketed expressions of Eq. (41), (42) and (43) are also simplified to scalar values

$$k_1 = \frac{\pi^2}{2}$$

$$k_2 = \frac{\left(24 - 2\pi^2\right)}{\pi^4}$$

$$k_3 = \frac{\left(\pi^4 + 45\right)}{240\pi^4}$$

and where

$\hat{q}_{LTRB,0}$ = one-mode approximate lateral-torsional-roll buckling load of a girder without major-axis deflection, prestressing, or overhangs

Subscript 0 indicates the same fidelity level as Mast's classical lateral-roll buckling solution.

Equation (44) can be rearranged algebraically in terms of two special case solutions, namely the one-mode lateral-roll buckling and lateral-torsional buckling solutions, to give insight into a solution form that can be useful for design. The lateral-roll buckling solution is found by setting $GJ \rightarrow \infty$ and solving Eq. (44). Similarly, lateral-torsional buckling is solved by setting $y_{r,eq} \rightarrow \infty$ (that is, infinite roll resistance at supports). The two results are given in Eq. (45) and (46).

$$\hat{q}_{LRB,0} = -\left(\frac{k_1}{k_2} \right) \left(\frac{EI_{yy} y_{r,eq}}{L^4} \right) = -113 \left(\frac{EI_{yy} y_{r,eq}}{L^4} \right) \tag{45}$$

where

$\hat{q}_{LRB,0}$ = one-mode approximation of classical lateral-roll-buckling load

$$\hat{q}_{LTB,0} = \sqrt{\left(\frac{k_1}{k_3} \right) \left(\frac{GJEI_{yy}}{L^6} \right)} = 28.4 \left(\frac{\sqrt{GJEI_{yy}}}{L^3} \right) \tag{46}$$

where

$\hat{q}_{LTB,0}$ = one-mode approximation of classical lateral-torsional buckling load

Again, $y_{r,eq}$ is less than 0 for the equivalent hanging case, and hence the critical lateral-roll buckling load is positive. In these expressions, the hat indicates the result of a truncated modal approximation whereas the subscript denotes that these results do not include major-axis deflection, prestressing, or overhangs. The one-mode lateral-torsional buckling coefficient of 28.4 is close to the classical solution,[25] which is approximately 28.3. This is because the assumed sinusoidal shape is close to the true lateral-torsional buckling mode shape for a simply supported beam with a distributed load.[25] The one-mode lateral-roll buckling coefficient of 113 is not as close to Mast's classical coefficient[6] of 120 from Eq. (11). Though the one-mode solution does not yield exact results, the Ritz-Galerkin method allows for the development of a solution form that is nearly exact, as follows.

A combination of Eq. (44), (45), and (46), with some rearrangement (and the fact that the center of gravity and center of twist align for doubly symmetric cross sections), produces Eq. (47).

$$\left(\frac{\hat{q}_{LTRB,0}}{\hat{q}_{LTB,0}}\right)^2 + \frac{\hat{q}_{LTRB,0}}{\hat{q}_{LRB,0}} = 1 \tag{47}$$

where

$q_{LTB,0}$ = classical lateral-torsional buckling load derived by Timoshenko and Gere

$q_{LRB,0}$ = classical lateral-roll buckling load derived by Mast

This interaction equation represents the transition of the one-mode approximate lateral-torsional-roll buckling load between roll-dominated behavior and twist-dominated behavior. It is hypothesized that the form of the interaction equation will prove sufficiently accurate for the exact, as opposed to the modal approximate, solution; and the inclusion of features such as major-axis bending, prestressing, and overhangs. The converged solution obtained using additional modes[24] shows that this hypothesis is not identically correct but that the error is small. Hence, the superscript hats indicating a modal approximation and the subscripts indicating the limited model fidelity can both be dropped to make Eq. (48), a generic interaction equation.

$$\left(\frac{q_{LTRB}}{q_{LTB}}\right)^2 + \frac{q_{LTRB}}{q_{LRB}} = 1 \tag{48}$$

where

q_{LTRB} = exact lateral-torsional-roll buckling load

q_{LTB} = exact lateral-torsional buckling load

q_{LRB} = exact lateral-roll buckling load

Figure 9 plots this interaction equation, which shows that torsional flexibility only reduces the buckling load slightly when lateral-roll buckling-type boundary conditions prevail (that is, q_{LTRB}/q_{LTB} is less than 0.1). The generic interaction equation can be used at any desired level of fidelity.

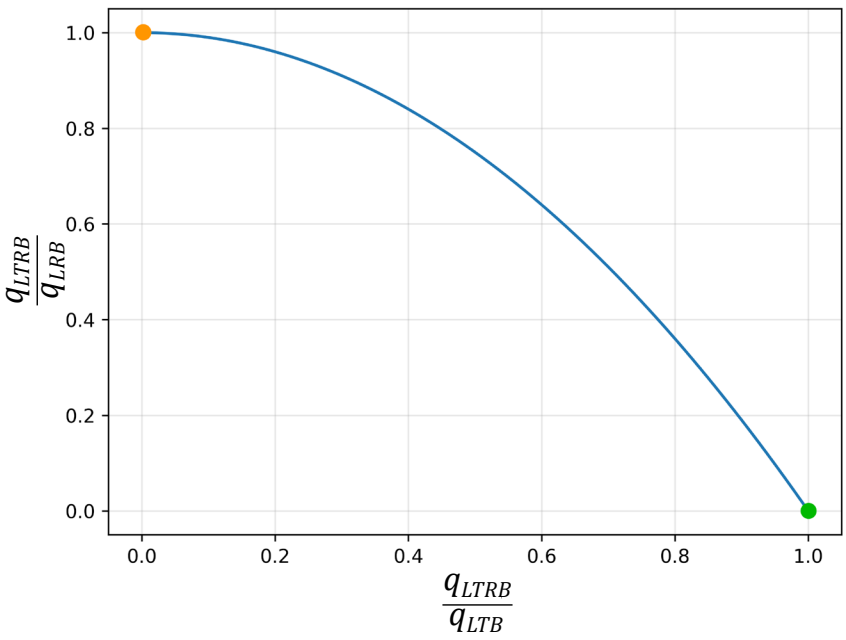

Figure 9. Effect of interaction between rigid-roll and relative twist on the lateral-torsional-roll buckling load. Note: q_{LRB} = exact lateral-roll buckling load; q_{LTB} = exact lateral-torsional buckling load; q_{LTRB} = lateral-torsional-roll buckling load from the near-exact interaction equation solution form.

Baseline lateral-torsional-roll buckling load without major-axis deformation, prestressing, or overhangs

If the classical lateral-roll buckling solution $q_{LRB,0}$[6] and the classical lateral-torsional buckling solution $q_{LTB,0}$[25] are used in the interaction Eq. (48), the quadratic interaction equation can be solved for the corresponding "basic" lateral-torsional-roll buckling load for an end-supported girder with no major-axis deflections $q_{LTRB,0}$. This can be rearranged as a torsion knockdown factor $g(\eta_0)$ that multiplies the well-known $q_{LRB,0}$ result. The knockdown factor isolates the effect of torsion on the buckling load and follows the same subscript convention already outlined for q. In other words, the functional forms of Eq. (49) and (50) do not change with higher levels of fidelity (to be introduced in the subsequent section).

$$q_{LTRB,0} = g(\eta_0) q_{LRB,0} \tag{49}$$

$$g(\eta_0) = \frac{2}{\eta_0}\left(\sqrt{1+\eta_0} - 1\right) \tag{50}$$

where

η_0 = torsion parameter for end-supported girder with rigid major axis

Equations (51) and (52) provide calculations for η_0.

$$\eta_0 = 71.0\beta^2 \tag{51}$$

$$\beta = \sqrt{\left(\frac{y_{r,eq}}{L}\right)^2 \left(\frac{EI_{yy}}{GJ}\right)} \tag{52}$$

The knockdown version of the lateral-torsional-roll buckling equations is particularly useful because the critical lateral-roll buckling load is easy to calculate and is already extensively used in current design procedures. Furthermore, the effects of roll and twist are separated and the dimensionless cross-sectional parameter β is easy to calculate. A β value of zero produces the lateral-roll buckling solution while large β values tend toward to the lateral-torsional buckling solution. **Figure 10** plots the basic case buckling loads ($q_{LRB,0}$, $q_{LTB,0}$, $q_{LTRB,0}$) normalized by the classical lateral-roll buckling solution, so that the blue curve represents the torsional knockdown factor. The figure indicates that β equal to 2 can practically be taken as the lateral-torsional buckling condition. Most precast concrete girders that require stability checks are characterized by a β value less than 0.1 while steel girders have a higher EI_{yy}/GJ ratio and will be characterized by larger β values. Practical considerations will be discussed in more detail in the "Example Application" section.

Incorporation of downward major-axis deflection and draped prestressing effects

As indicated by the subscript 0 in Eq. (49), the knockdown factor plotted in Fig. 10 is specific to end-supported girders where the major-axis bending and prestressing upwards displacement are negligible. These approximations permitted a tractable

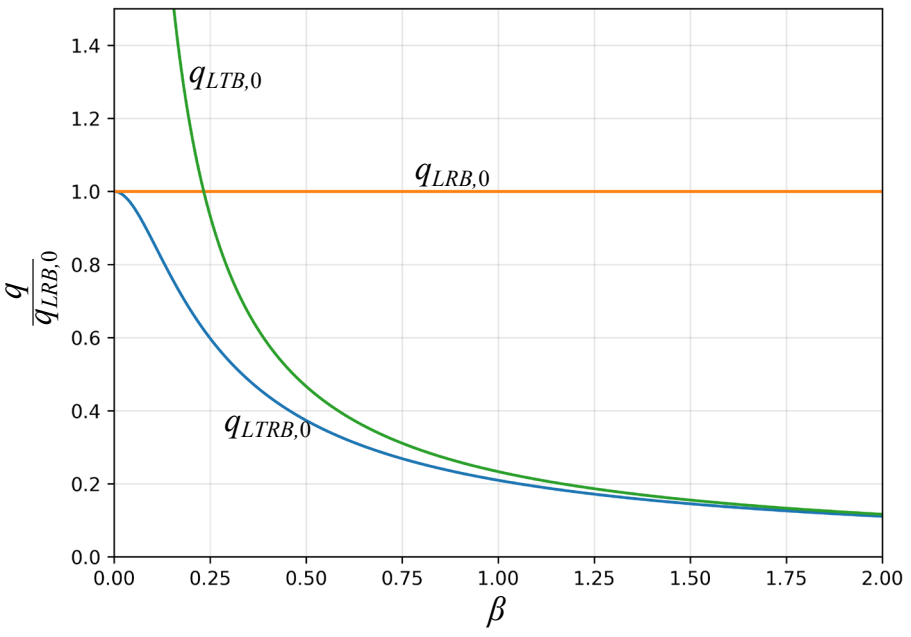

Figure 10. Effect of unitless cross-sectional parameter β on the level of interaction between lateral-roll buckling and lateral-torsional buckling basic solutions. Note: $q_{LRB,0}$ = classical lateral-roll buckling load derived by Mast; $q_{LTB,0}$ = classical lateral-torsional buckling load derived by Timoshenko and Gere; $q_{LTRB,0}$ = basic lateral-torsional-roll buckling load.

Ritz-Galerkin formulation (that is, formulation with one-mode shape function approximation). However, the usefulness of the interaction equation in Eq. (48), which is nearly general, is that it can also accommodate higher fidelity lateral-roll buckling and lateral-torsional buckling solutions. Although some of these lateral-roll buckling solutions were summarized previously, the higher-fidelity lateral-torsional buckling solutions can be difficult to find and are often in the form of a series solution, giving the corresponding knockdown equation a form that is unsuitable for presentation here. For demonstration's sake, the interaction form is specialized here with an approximate form of the higher-fidelity lateral-torsional buckling component. (Ultimately, the user should exercise discretion to choose appropriate and consistent lateral-roll buckling and lateral-torsional buckling solutions to be used within the interaction equation.)

To include the effects of major-axis deflections and prestressing upwards displacement in the lateral-torsional buckling component, the solution of Vacharajittiphan et. al[28] is used, plus the additional assumption of no warping restraint. Further, if GJ/EI_{xx} is taken as zero (**Table 1**), then Eq. (53) provides the lateral-torsional buckling load of an end-supported girder with major-axis deflections due to gravity and prestressing $q_{LTB,vp}$.

$$q_{LTB,vp} \cong q_{LTB,v} = q_{LTB,0}\sqrt{\frac{1}{1-\frac{I_{yy}}{I_{xx}}}} \tag{53}$$

where

$q_{LTB,v}$ = lateral-torsional buckling load of an end-supported girder with major-axis deflections due to gravity

The approximation that $q_{LTB,vp}$ is equal to $q_{LTB,v}$ relies on analysis by Peart et al.[19] that indicates a limited effect of camber on the lateral-torsional buckling load, although it is not clear that this should always be the case. For prestressed concrete girders, the lateral-torsional buckling load is typically much higher than the lateral-roll buckling load, in which case minor errors in the lateral-torsional buckling load have little effect on the critical (lateral-torsional-roll buckling) load.

Using $q_{LRB,vp}$ from Eq. (21) and $q_{LTB,vp}$ from Eq. (53) within the interaction equation, the resulting knockdown equation is of the same form as Eq. (49), (50), (51), and (52) but with a modified torsion parameter for an end-supported girder with major-axis deflections due to gravity and prestressing η_{vp}, given in Eq. (54).

$$\eta_{vp} = \eta_0 \frac{\left(1-\frac{\overline{v}_{loc,p}}{y_{r,eq}}\right)^2}{1-\frac{I_{yy}}{I_{xx}}} \tag{54}$$

Substituting Eq. (54) into Eq. (50) yields the knockdown expression for the lateral-torsional-roll buckling load of an end-supported girder with major-axis deflections due to gravity and prestressing, $q_{LTRB,vp} = g(\eta_{vp})q_{LRB,vp}$, where $g(\eta_{vp})$ is the torsion knockdown factor for an end-supported girder with major-axis flexibility and prestress upwards deflection = $\frac{2}{\eta_{vp}}\left(\sqrt{1+\eta_{vp}}-1\right)$.

Incorporation of overhangs

In this section, the critical load will be extended to incorporate overhangs, again using the interaction equation. From Eq. (27), the effect of overhangs on the lateral-roll buckling load is given by Eq. (55).

$$q_{LRB,vp\alpha} = \frac{q_{LRB,vp}}{f_{LRB}\left(\alpha,t\right)} \tag{55}$$

Table 1. Section properties and torsional parameters for various Washington State Department of Transportation wide flange series girders

h, in.	$L_{LTRB,vp\alpha}$, ft	L/h	J, in.4	I_{yy}, in.^{4}	I_{yy}/I_{xx}	EI_{yy}/GJ	GJ/EI_{xx}	$y_{r,eq}$, in.	r_{yy}, in.	β	$g(\eta_{vp\alpha})$
74	210	34.0	18,400	72,370	0.09883	9.45	0.0105	-38.4	8.85	0.0467	0.942
83	215	31.1	19,100	72,550	0.07499	9.13	0.0082	-43.0	8.61	0.0499	0.924
95	221	27.8	19,900	72,770	0.05420	8.74	0.0062	-49.2	8.31	0.0546	0.899
100	223	26.7	20,400	72,870	0.04791	8.58	0.0056	-51.8	8.20	0.0565	0.890
120	228	22.8	21,900	73,250	0.03086	8.03	0.0039	-62.0	7.79	0.0640	0.854
150	232	18.5	24,200	73,830	0.01796	7.32	0.0025	-77.3	7.29	0.0749	0.804

Note: Torsional parameters and buckling length are calculated for a consistent safety factor of 1.5. q_p/q_{sw} = -2.0. 1 in = 25.4 mm; 1 ft = 0.305 m; 1 lb = 4.448 N. EI_{xx} = major-axis flexural rigidity; EI_{yy} = minor-axis flexural rigidity; $g(\eta_{vp\alpha})$ = torsion knockdown factor with major-axis flexibility, prestress uplift, and overhangs; GJ = torsional rigidity; h = girder depth; I_{xx} = major-axis second moment of area; I_{yy} = minor-axis second moment of area; J = second polar moment of area; L = total girder length; $L_{LTRB,vp\alpha}$ = lateral-torsional-roll buckling length for asymmetrically supported girder with major-axis deflections from gravity and prestressing; q_p = nominal prestressing load, idealized as uniformly distributed load (typically upward, and therefore negative); q_{sw} = uniform (prismatic) girder self-weight; r_{yy} = minor-axis radius of gyration; w_c = concrete density = 155 lb/ft^3; $y_{r,eq}$ = equivalent hanging distance; β = unitless cross-sectional parameter.

Likewise, a function $f_{LTB}(\alpha,t)$ should respect the form of Eq. (56).

$$q_{LTB,vp\alpha} = \frac{q_{LTB,vp}}{f_{LTB}(\alpha,t)} \quad (56)$$

where

$q_{LTB,vp\alpha}$ = lateral-torsional buckling load of a girder with asymmetric overhangs and major-axis deflections due to gravity and prestressing

Substituting the above two expressions into the interaction expression in Eq. (48) gives Eq. (57).

$$\left(\frac{q_{LTRB,vp\alpha}}{q_{LTB,vp}/f_{LTB}(\alpha,t)}\right)^2 + \left(\frac{q_{LTRB,vp\alpha}}{q_{LRB,vp}/f_{LRB}(\alpha,t)}\right) = 1 \quad (57)$$

where

$q_{LTRB,vp\alpha}$ = lateral-torsional-roll buckling load of a girder with asymmetric overhangs and major-axis deflections due to gravity and prestressing

$f_{LTB}(\alpha,t)$ = overhang factor for girder with full twist-restraint at supports

A near-exact approximation for the overhang factor for girder with full twist-restraint at supports $f_{LTB}(\alpha,t)$ can be obtained by assuming that overhangs provide minimal warping restraint so that the girder with overhangs can be treated as an equivalent simply supported girder of length $(1 - \alpha_1 - \alpha_2)L$. This assumption should be valid for overhangs less than about 0.2 times the span, which approximately corresponds to the critical point already noted for lateral-roll buckling overhangs in Fig. 8. For larger overhangs, cantilever-type behavior dominates, and it is unclear what form the true lateral-torsional buckling overhang factor takes. However, for moderate overhangs the lateral-torsional buckling uniform load q_{LTB} is proportional to $1/span^3$.

$$q_{LTB,vp\alpha} = \frac{q_{LTB,vp}}{(1-\alpha_1-\alpha_2)^3} \quad (58)$$

Equating Eq. (56) and (58) and keeping with the form of Eq. (25) gives Eq. (59).

$$f_{LTB}(\alpha,t) = \sum_{j=0}^{4} b_{LTB,j}\alpha_m^j \quad (59)$$

where

$b_{LTB,j}$ = coefficients for polynomial order j in the lateral-torsional buckling overhang factor = [+1, -6, +12, -8, 0] (calculated by expanding the denominator of Eq. [58])

Solving the quadratic Eq. (57), and with significant reorganization, it can be shown that the torsion knockdown factor $g(\eta_{vp\alpha})$ has the same functional form already derived for lower fidelity levels, giving Eq. (60).

$$q_{LTRB,vp\alpha} = g(\eta_{vp\alpha})q_{LRB,vp\alpha} \quad (60)$$

where

$g(\eta_{vp\alpha})$ = torsion knockdown factor of a girder with major-axis flexibility, prestress uplift, and asymmetric overhangs

Equation (61) calculates the torsion parameter of a girder with asymmetric overhangs and major-axis deflections due to gravity and prestressing $\eta_{vp\alpha}$.

$$\eta_{vp\alpha} = \eta_{vp}\left[\frac{f_{LTB}(\alpha,t)}{f_{LRB}(\alpha,t)}\right]^2 \quad (61)$$

If desired, the overhang factor for an asymmetrically supported, torsionally flexible girder $f_{LTRB}(\alpha,t)$ can be determined from the definition of the overhang factor in Eq. (62).

$$q_{LTRB,vp\alpha} = \frac{q_{LTRB,vp}}{f_{LTRB}(\alpha,t)} \quad (62)$$

Noting the equivalency of Eq. (60) and (62), plus the substitution of Eq. (27) gives Eq. (63).

$$f_{LTRB}(\alpha,t) = \left(\frac{f_{LTB}^2(\alpha,t)}{f_{LRB}(\alpha,t)}\right)\left(\frac{\sqrt{1+\eta_{vp}}-1}{\sqrt{1+\eta_{vp\alpha}}-1}\right) \quad (63)$$

Equation (63) collapses to the lateral-roll buckling or lateral-torsional buckling subcase for the associated limiting β values. Unlike $f_{LRB}(\alpha,t)$ and $f_{LTB}(\alpha,t)$, the lateral-torsional-roll buckling overhang factor depends not only on the overhang distances but also on the dimensionless parameter β, the major-axis flexibility ratio I_{yy}/I_{xx}, and the cambering ratio $\overline{v}_{loc,p}/y_{r,eq}$ (included within η). For the special case of q_p equal to $-q_{sw}$, η_{vp} collapses to η_0 and $f_{LTRB}(\alpha,t)$ is bounded by the lateral-roll buckling and lateral-torsional buckling limit cases only as a function of β. **Figure 11** shows this, where the overhang stabilizing effect $1/f_{LTRB}(\alpha,t)$ is plotted against the symmetric overhang ratio. The orange lateral-roll buckling curve corresponds to the t equals 0 curve of Fig. 8. For real girders (β greater than 0), the influence of torsion reduces the stabilizing effect of overhangs. The results closely match those by Peart et al.[17] for α values up to 0.15. However, the results of Peart et al. are presented as a sixth-order truncation, which appears to perform poorly for larger overhang values. Peart et al.'s values do not converge to the lateral-roll buckling solution when β equals 0. Unlike the result from Peart et al., Eq. (63) is not limited to symmetric overhangs. It is, however, limited by the assumption on lateral-torsional buckling overhang behavior, which becomes less valid for long overhangs. To reflect this, the curves in Fig. 11 are dashed beyond α_m equal to 0.2, which is also a practical upper limit for overhangs.

Example application: stability during handling of WSDOT WF girders

To give readers a sense of the effects of torsional deformations on lateral stability, this discussion focuses on the lateral-torsion-

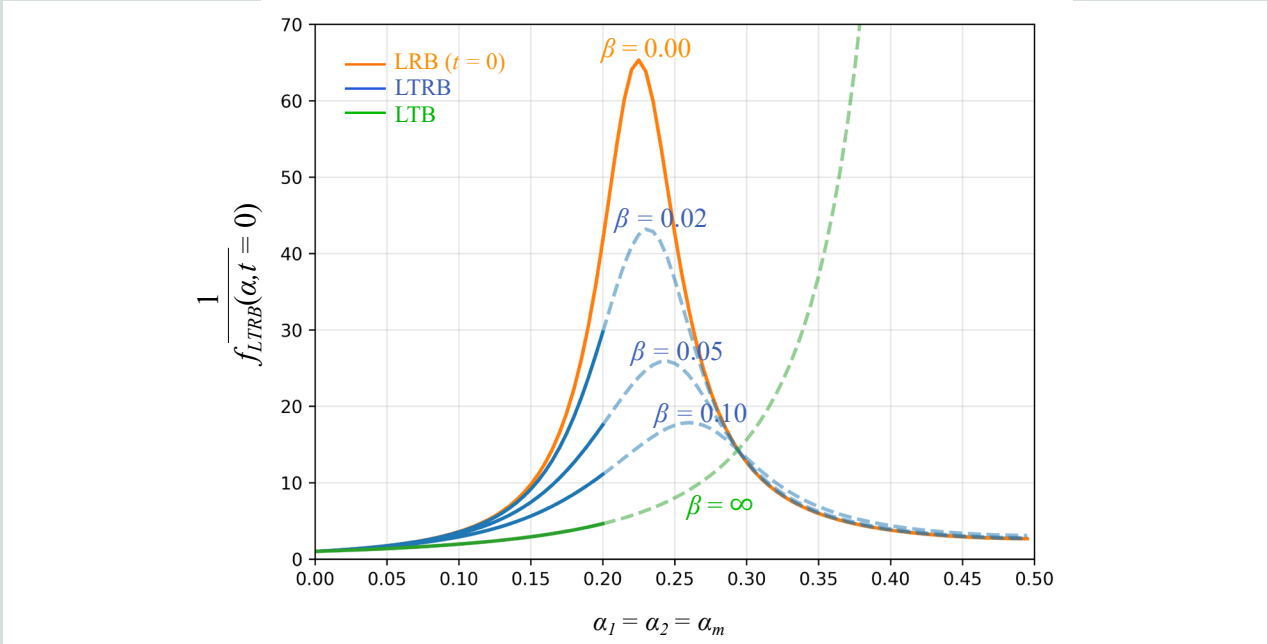

Figure 11. Overhang stabilization effect is reduced from the pure lateral-roll buckling case due to torsional influence. Results shown here are for the special case for which q_p equals $-q_{sw}$ (color plot online). Note: $f_{LTRB}(\alpha,t)$ = overhang factor for asymmetrically supported, torsionally flexible girder ; *LRB* = lateral-roll buckling; *LTB* = lateral-torsional buckling; *LTRB* = lateral-torsional-roll buckling ; q_p = nominal prestressing load, idealized as uniformly distributed load (typically upward, and therefore negative); q_{sw} = uniform (prismatic) girder self-weight; t = girder's level of asymmetry; α_m = mean overhang ratio; α_1 = overhang ratio at end 1; α_2 = overhang ratio at end 2; β = unitless cross-sectional parameter.

al-roll buckling conditions for real girder profiles. To this end, the common WSDOT WF (wide-flange) girder series is studied because it is among the most structurally efficient prestressed concrete girder shapes used in the United States. All girders in the WF series have the same flange dimensions, allowing identical flange formwork to be used for any girder depth. Deeper girders are formed simply by adding an extra piece to the web form. **Figure 2** shows a typical WF girder cross section.

Stability analysis is performed for a hanging girder with 10% overhangs at each end, and with a tendon profile that produces an equivalent uniform prestressing load q_p equal to $-2.0q_{sw}$. Analysis is performed for a range of girder depths to evaluate the trend in the torsional knockdown factor as deeper girders are used on longer spans. For a given section depth, the girder length is determined by maintaining a consistent safety factor of 1.5 against buckling.

Consideration is also given to the effect of using lightweight concrete, which may be needed to satisfy weight limits when hauling long girders. Relative to a normalweight 155 lb/ft^3 (2490 kg/m^3) concrete girder, a lightweight 125 lb/ft^3 (2000 kg/m^3) concrete girder will have lower self-weight but will also be characterized by a lower modulus of elasticity. The decrease in self-weight and reduction of the modulus of elasticity will produce opposite effects for the lateral-torsional-roll buckling load and length. Concrete modulus of elasticity E_c is derived from the concrete density w_c according to the American Association of State Highway and Transportation Officials' *AASHTO LRFD Bridge Design Specifications*,[29] where Eq. (64) shows that the modulus decay outpaces the weight savings. This would indicate that the use of lightweight concrete will decrease stability, all else remaining equal.

$$E_c = 120{,}000 w_c^2 f_c'^{\,0.33} \tag{64}$$

where

f_c' = concrete cylinder compressive strength at 28 days, with units of ksi in Eq. (64)

w_c = concrete density, with units of kip/ft^3 in Eq. (64)

A concrete strength of 9 ksi (62 MPa) is used in this example. The ratio of the concrete modulus of elasticity to concrete shear modulus E_c/G_c is $2(1 + \upsilon)$, where υ is Poisson's ratio and is assumed to equal 0.2 for concrete.

Girder section properties are calculated for a range of section depths from 74 to 150 in., even if such girders are not currently used in practice. (The deepest section commonly available is 100 in. [2540 mm].) In the calculation of $y_{r,eq}$, any extension of the lifting loops above the top flange is ignored. Calculation of the second polar moment of area J is performed according to the procedure of Martin,[30] who subdivided a cross section into several trapezoidal regions and summed their

contributions. If more-accurate calculations are required, the Prandtl membrane analogy can be implemented in a computer program, as outlined by Yoo.[31] Some cross-section parameters are tabulated in Table 1 for commonly available WF sections (WF74G, WF83G, WF95G, WF100G) as well as some hypothesized deeper sections (WF120G, WF150G). Spot checks showed that, for results in Table 1, J values are within 5% of the Prandtl solution.

Table 1 also shows the output of the buckling calculations for the WF girders. For the consistent safety factor condition, the knockdown factor $g(\eta_{vp\alpha})$ decreases with increasing span. This means that torsional deformations cause a relatively greater reduction in the critical load for longer spans. In an approximate sense, this can be seen by expanding Eq. (49) (or analogous) in a Taylor series and truncating (because η is much less than 1.0 for practical configurations). For the basic case, this gives Eq. (65).

$$g\left(\eta_0(\beta)\right) \approx 1 - 18\beta^2 = 1 - 18\left(\frac{y_{r,eq}}{L}\right)^2\left(\frac{EI_{yy}}{GJ}\right) \tag{65}$$

For girders such as the WSDOT series, which use the same

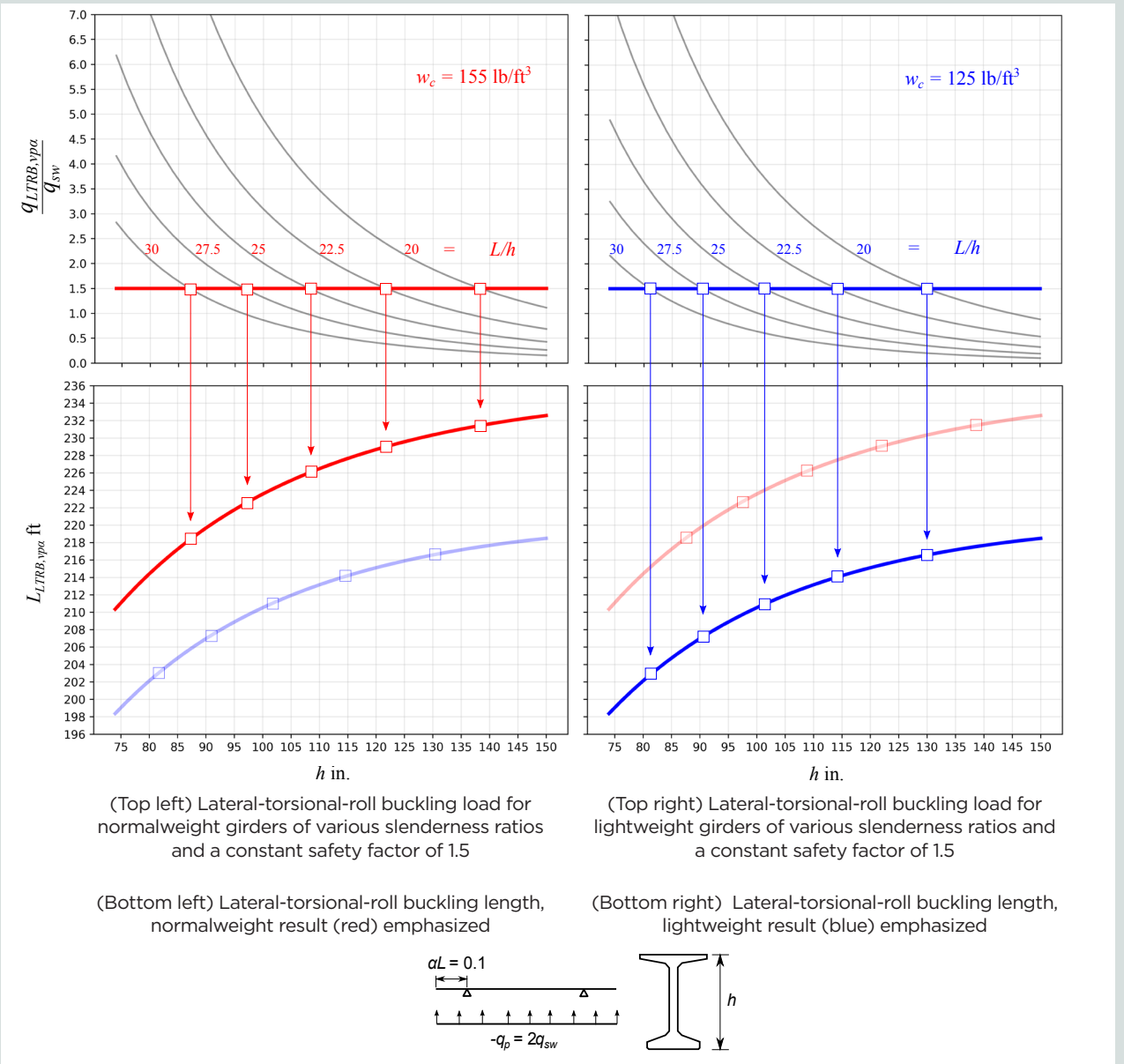

(Top left) Lateral-torsional-roll buckling load for normalweight girders of various slenderness ratios and a constant safety factor of 1.5

(Top right) Lateral-torsional-roll buckling load for lightweight girders of various slenderness ratios and a constant safety factor of 1.5

(Bottom left) Lateral-torsional-roll buckling length, normalweight result (red) emphasized

(Bottom right) Lateral-torsional-roll buckling length, lightweight result (blue) emphasized

Figure 12. Lateral-torsional-roll buckling of Washington State Department of Transportation WF series girders. Note: h = girder depth; L = total girder length; $q_{LTRB,vp\alpha}$ = lateral-torsional-roll buckling load of a girder with asymmetric overhangs and major-axis deflections due to gravity and prestressing; q_p = nominal prestressing load, idealized as uniformly distributed load (typically upward, and therefore negative); q_{sw} = uniform (prismatic) girder self-weight; w_c = concrete density; α = ratio of overhang distance to total girder length. 1 in = 25.4 mm; 1 ft = 0.305 m; 1 lb = 4.448 N.

top and bottom flange forms for several girder depths, EI_{yy} and GJ change little with depth. Most of the reduction in $g(\eta_0)$ (or analogous) therefore comes from the change in the span-to-depth ratio, and consequently the ratio $y_{r,eq}/L$.

The critical load is calculated using the torsion knockdown factor via Eq. (60). The load is then normalized by the self-weight and plotted against the girder depth h in **Fig. 12** for normalweight concrete (in red). Results are plotted for various L/h ratios and are overlayed with a horizontal line at 1.5, indicating a consistent safety factor constraint. Values reported in Table 1 would lie along this line (but are not directly indicated). Figure 12 shows that deeper, and hence longer, girders require lower ratios of L/h (that is, shorter spans) to satisfy the consistent safety factor constraint. Many precast and prestressed concrete girders in practice have $L/h \approx 25$, based on service stresses; however, for deeper sections, this ratio must be limited because such a section will be controlled by stability during handling rather than by allowable stresses under initial and service loads. Figure 12 shows (in red) the girder lengths at buckling by directly translating from the intersection points in the top figure. There are diminishing returns on the critical length as the depth of the WF sections is increased. In other words, added section depth is ineffective in preventing stability issues.

Some insight can be gained into the key cross-sectional parameters that control girder stability, therefore indicating parameters that improve stability more efficiently than depth. Because complexities due to camber are not at the cross-section level, the basic lateral-torsional-roll buckling Eq. (49), (50), (51), and (52) suffice for this discussion; they are rearranged along with Eq. (14) via the substitutions:

$$q_{sw} = Aw_c, I_{yy} = Ar_{yy}^2, y_{r,eq} \cong \frac{h}{2}$$

where

A = girder cross-sectional area

r_{yy} = minor-axis radius of gyration

This results in Eq. (66), an approximate expression for the lateral-torsional-roll buckling length for the basic case with symmetric overhangs.

$$\frac{q_{LTRB,0}}{q_{sw}} \approx \left(\frac{60}{L}\right)\left(\frac{E_c}{w_c}\right)\left(\frac{h}{L}\right)\left(\frac{r_{yy}}{L}\right)^2\left[\frac{g(\eta_0)}{f_{LRB}(\alpha)}\right] \qquad (66)$$

In Eq. (66), the units must be consistent. The variables are grouped for ease of evaluation. To a first approximation, if the material properties (embedded in E_c/w_c), span-to-depth ratio L/h, and overhang ratio α are kept the same, then the safety factor against lateral-torsional-roll buckling is proportional to r_{yy}^2 / L^3. To maintain a consistent safety factor for longer spans, r_{yy} would therefore have to be proportional to $L^{1.5}$, or the overhang ratio would have to be increased. The former implies a significant increase in top-flange width, which would increase trucking weight, whereas the latter would at least require more temporary top strand and may also pose challenges at particular phases in the erection sequence. For example, when the girder is first set on the pier cap it might become end-supported with no overhang. In a more precise estimate, r_{yy} should be proportional to L raised to a power slightly higher than 1.5, because the factor $g_0(\eta_0)$ decreases (the torsional deformations exact a greater toll) as the span increases. The best girder profile for longer girders needs to be investigated and will need to account for many criteria in addition to stability, but such an investigation lies outside the scope of this study.

The effect of using lightweight concrete can be deduced from the ratio E_c/w_c, which appears in Eq. (66). According to the AASHTO LRFD specifications,[29] E_c is proportional to w_c^2, in which case the ratio E_c/w_c is proportional to w_c. The safety factor against buckling then increases for heavier concretes and decreases for lightweight concrete. Figure 12 shows this finding, where a lightweight concrete curve (blue) is overlaid on the normalweight concrete (red) results. Thus, if lightweight concrete is used, the design must compensate for the reduction in safety against buckling.

Summary

This study represents the first step in a reexamination of current methods for lateral stability analysis of long prestressed concrete girders. An important step in stability analysis is the evaluation of initial imperfection amplifications, but to do that, the critical load must be known. This article addresses the critical load, focusing on the elastic buckling load of girders in the hanging condition, which is the most critical scenario due to the lack of end-twist restraint. Girders that are supported from below can be evaluated as equivalent hanging girders.

The classical lateral-roll buckling analysis by Mast[6] was augmented to include the effect of major-axis deflections and asymmetric overhangs. Although asymmetric overhangs are most likely to occur during girder trucking, the problem boundary conditions were formulated so that the trucking condition can easily be transformed into an equivalent hanging girder. For practical lifting-point locations, the asymmetric formulation can safely be replaced by the simpler, symmetric equation, using the average overhang length.

Torsional deformations were included in the solution of the classical governing differential equation for twist of a simply supported beam by enforcing compatibility between support rotations and torque reactions. No closed-form solution exists for this problem, but a near-exact solution with all deformations included was found for the lateral buckling load of an end-supported beam by employing a Ritz-Galerkin solution technique. From a single-term approximation for the twist shape function, it was possible to develop a buckling equation in the form of an interaction equation between two special cases: lateral-roll buckling and lateral-torsional buckling. Consideration of torsional deformations reduces the buckling load when all other parameters remain the same. The reduction increases with length (for a consistent safety factor

against buckling) and can be calculated as a knockdown factor that is separable from lateral bending.

A simplified form of this equation shows the variables at play in lateral-torsional-roll buckling, in their appropriate powers, from which it is seen that lightweight concrete reduces lateral buckling stability.

Conclusion

The advent of high-performing concrete materials along with urban congestion has led to prestressed concrete girders that need to span longer distances and so are increasingly slender. Traditionally, a designer's recourse against stability problems is to increase the lateral resistance, either through cross-section modifications or by reducing the effective span via overhangs. These remediation measures may not be as effective as suggested by the existing design equations. This concern is related to torsional flexibility, which has the following effects on lateral stability:

- Torsional deformations reduce the buckling load when all other parameters remain the same. The reduction increases with length.
- Major-axis bending affects lateral-torsional-roll buckling stability slightly. Similar to lateral-roll buckling, downward gravity deflections raise the buckling load while net upward camber lowers it. These major-axis effects are amplified in the presence of torsion.
- Although bringing the lifting points in from the ends (that is, producing overhangs) greatly improves lateral stability, this benefit is tempered by torsional flexibility. In other words, the classical lateral-roll buckling overhang stabilization factor is slightly unconservative for the torsional case. The difference is small for overhangs less than 10%, but it becomes apparent for longer girders with larger overhangs.
- The minor-axis radius of gyration r_{yy} is the most important cross-sectional parameter controlling stability. For a constant safety factor, it must be proportional to $L^{1.5}$. As girder spans continue to increase, new cross-section shapes that respect this relationship may be desirable.
- The use of lightweight concrete reduces the applied load (the girder weight) but also reduces the buckling load. The net effect is to reduce the safety factor against buckling.

References

1. West, C. 2019. "Prestressed Concrete Girders Achieve Record Lengths." *Aspire* 13 (4): 56–57.
2. Washington State Department of Transportation. 2020. "Standard Design Drawings." https://wsdot.wa.gov/eesc/bridge/designmemos/14-2008.htm.
3. Oesterle, R. G., M. J. Sheehan, H. R. Lotfi, W. G. Corley, and J. J. Roller. 2007. *Investigation of Red Mountain Freeway Bridge Girder Collapse*. Final report. CTLGroup project 262291. Skokie, IL: CTLGroup.
4. Rose, J. 2013. "Marquam Bridge Wreck Likely Caused by Truck with Massive Beam Braking for Portland Traffic Jam." *The Oregonian*. April 24, 2013. https://www.oregonlive.com/commuting/2013/04/crippling_marquam_bridge_wreck.html.
5. Zureick, A. H., L. F. Kahn, K. M. Will, I. Kalkan, J. Hurff, and J. H. Lee. 2009. *Stability of Precast Prestressed Concrete Bridge Girders Considering Sweep and Thermal Effects*. Final report. GDOT project no. 05-15. Georgia Department of Transportation. https://www.dot.ga.gov/BuildSmart/ResearchDocuments/05-15.pdf.
6. Mast, R. F. 1989. "Lateral Stability of Long Prestressed Concrete Beams, Part 1." *PCI Journal* 34 (1): 34–53. https://doi.org/10.15554/pcij.01011989.34.53.
7. PCI. 2020. *User Manual for Calculating the Lateral Stability of Precast, Prestressed Concrete Bridge Girders*. CB-04-20. Chicago, IL: PCI. https://doi.org/10.15554/CB-04-20.
8. FHWA (Federal Highway Administration). 2015. *Engineering for Structural Stability in Bridge Construction.* Report FHWA-NHI-15-044, Washington, DC: FHWA. https://www.fhwa.dot.gov/bridge/pubs/nhi15044.pdf.
9. Lebelle, P. 1959. "Stabilite Elastique des Poutres en Beton Precontrain a L'Egard du Deversement Lateral." *Annales de L'Institut Technique du Batiment et des Travaux Publics* 12 (141): 778–831.
10. Swann, R. A., and W. G. Godden. 1966. "The Lateral Buckling of Concrete Beams Lifted by Cables." *The Structural Engineer*, no. 44, 21–33.
11. Anderson, A. R. 1971. "Lateral Stability of Long Prestressed Concrete Beams." *PCI Journal* 16 (3): 7–9.
12. Mast, R. F. 1993. "Lateral Stability of Long Prestressed Concrete Beams, Part 2." *PCI Journal* 38 (1): 70–88. https://doi.org/10.15554/pcij.01011993.70.88.
13. PCI. 2016. *Recommended Practice for Lateral Stability of Precast, Prestressed Concrete Bridge Girders*. CB-02-16. Chicago, IL: PCI.
14. Stratford, T. J., and C. J. Burgoyne. 1999. "Lateral Stability of Long Precast Concrete Beams." *Structures and Buildings* (Proceedings of the Institution of Civil Engineers) 134 (2): 169–180. https://doi.org/10.1680/istbu.1999.31383.

15. Stratford, T. J., and C. J. Burgoyne. 2000. "The Toppling of Hanging Beams." *International Journal of Solids and Structures* 27 (26): 3569–3589. https://doi.org/10.1016/S0020-7683(99)00059-1.

16. Stratford, T. J., C. J. Burgoyne, and H. P. J. Taylor. 1999. "Stability Design of Long Precast Concrete Beams." *Structures and Buildings* (Proceedings of the Institution of Civil Engineers) 134 (2): 159–169. https://doi.org/10.1680/istbu.1999.31382.

17. Cojocaru, R. 2012. "Lifting Analysis of Precast Prestressed Concrete Beams," MS thesis, Virginia Polytechnic Institute and State University, Blacksburg, VA.

18. Plaut, R. H., and C. D. Moen. 2013. "Analysis of Elastic, Doubly Symmetric, Horizontally Curved Beams During Lifting." *Journal of Structural Engineering* 139 (1): 39–46. https://doi.org/10.1061/(ASCE)ST.1943-541X.0000612.

19. Peart, W. L., E. J. Rhomberg, and R. W. James. 1992. "Buckling of Suspended Cambered Girders." *Journal of Structural Engineering* 118 (2): 505–528. https://doi.org/10.1061/(ASCE)0733-9445(1992)118:2(505).

20. Pi, Y. L., and N. S. Trahair. 1992. "Prebuckling Deflections and Lateral Buckling. II: Applications." *Journal of Structural Engineering* 118 (11): 2967–2985. https://doi.org/10.1061/(ASCE)0733-9445(1992)118:11(2967).

21. Trahair, N. S., and S. T. Woolcock. 1973. "Effect of Major Axis Curvature on I-beam Stability." *Journal of Engineering Mechanics* 99 (1). https://doi.org/10.1061/JMCEA3.0001731.

22. Kitipornchai, S., and N. S. Trahair. 1980. "Buckling Properties of Monosymmetric I-beams." *ASCE Journal of the Structural Division* 106 (5). https://doi.org/10.1061/JSDEAG.0005441.

23. AISC (American Institute of Steel Construction). 2016. *Specification for Structural Steel Buildings*. ANSI/AISC 360-16. Chicago, IL: https://doi.org/10.1061/JSDEAG.0005441.

24. ASME (American Society of Mechanical Engineers). 2014. *Design of Below-the-Hook Lifting Devices*. BTH-1-2014. New York, NY: ASME.

25. Timoshenko, S. P., and J. M. Gere. 1961. *Theory of Elastic Stability*. New York, NY: McGraw-Hill.

26. Anderson, J. M., and N. S. Trahair. 1972. "Stability of Monosymmetric Beams and Cantilevers." *ASCE Journal of the Structural Division* 98 (1): 269–286. https://doi.org/10.1061/JSDEAG.0003114.

27. Galik, W. D., J. F. Stanton, and R. Wiebe. 2022. "Lateral-Torsional-Roll Stability of Long Precast Girders." Final report, University of Washington, Seattle, WA: PCI.

28. Vacharajittiphan, P., S. T. Woolcock, and N. S. Trahair. 1974. "Effect of In-plane Deformation on Lateral Buckling." *Journal of Structural Mechanics* 3 (1): 29–60. https://doi.org/10.1080/03601217408907255.

29. AASHTO (American Association of State Highway and Transportation Officials). 2020. *AASHTO LRFD Bridge Design Specifications* (customary U.S. units), 9th ed. Washington, DC: AASHTO.

30. Martin, R. C. 1969. "A Torsional Investigation of a Concrete I-Girder," master's thesis, Oregon State University.

31. Yoo, C. H. 2000. "Torsional and Other Properties of Prestressed Concrete Sections." *PCI Journal* 45 (3): 66–72. https://doi.org/10.15554/pcij.05012000.66.72.

Notation

$\{\hat{a}\}$ = coefficients of the *m*th modal twist shape approximation function collected into a column vector

$\{\overline{a}\}$ = weighting coefficients of the *m*th modal weight function, collected into a column vector

$\{\hat{a}_m\}$ = coefficients of the *m*th modal twist shape approximation function

A = girder cross-sectional area

$b_{LRB,j}$ = coefficients for polynomial order *j* in the lateral-roll buckling overhang factor

$b_{LTB,j}$ = coefficients for polynomial order *j* in the lateral-torsional buckling overhang factor

$[B_0]$ = derivative of the girder-twist shape function matrix $[N]$ with respect to ζ, evaluated at $\zeta = 0$

$\overline{c}_x$ = compliance coefficient for minor-axis deflection

$\overline{c}_{x,a}$ = compliance coefficient for minor-axis deflection of a girder with overhangs

$\overline{c}_y$ = compliance coefficient for major-axis deflection

$\overline{c}_{y,a}$ = compliance coefficient for major-axis deflection of a girder with overhangs

e_x = lifting loop eccentricity (positive in + x direction)

E = modulus of elasticity

E_c = concrete modulus of elasticity

EI_{xx} = major-axis flexural rigidity

EI_{yy} = minor-axis flexural rigidity

$f_{LRB}(\alpha)$ = overhang factor for symmetrically supported, torsionally rigid girder

$f_{LRB}(\alpha,t)$ = overhang factor for an asymmetrically supported, torsionally rigid girder

$f_{LTB}(\alpha,t)$ = overhang factor for girder with full twist-restraint at supports

$f_{LTRB}(\alpha,t)$ = overhang factor for asymmetrically supported, torsionally flexible girder

f_c' = concrete cylinder compressive strength at 28 days

$g(\eta_{vp})$ = torsion knockdown factor of an end-supported girder with major-axis flexibility and prestress uplift

$g(\eta_{vp\alpha})$ = torsion knockdown factor of a girder with major-axis flexibility, prestress uplift, and asymmetric overhangs

$g(\eta_0)$ = torsion knockdown factor for an end-supported girder with rigid major axis

G = shear modulus

G_c = concrete shear modulus

GJ = torsional rigidity

h = girder depth

I = second moment of area

I_{xx} = major-axis second moment of area

I_{yy} = minor-axis second moment of area

j = index representing the polynomial degree of α in each term of the overhang factor

J = second polar moment of area

$k_1 = \dfrac{\pi^2}{2}$

$k_2 = \dfrac{\left(24-2\pi^2\right)}{\pi^4}$

$k_3 = \dfrac{\left(\pi^4+45\right)}{240\pi^4}$

K_{tot} = special case of $[K_{tot}]$ for one-mode result

$[K_{tot}]$ = weak-form coefficient matrix for M mode approximation of girder twist

K_θ = total rotational stiffness (at the center of gravity) due to stiffness at the support and the lifting loops

$K_{\theta,sup}$ = support rotational stiffness due to rotational bearing or truck stiffness

$[K_1]$ = integral of the product of the shape function transpose matrix and its second derivative

$[K_2]$ = integral of the product of the shape function transpose matrix, its first derivative evaluated at the girder end, and the square of the major-axis bending moment shape

$[K_3]$ = integral of the product of the shape function matrix, its transpose, and the square of the major-axis bending moment shape

L = total girder length

$L_{LTRB,vp\alpha}$ = lateral-torsional-roll buckling length for asymmetrically supported girder with major-axis deflections from gravity and prestressing

M = number of mode shapes included in the twist approximation

$M_{z,loc}$ = internal girder moment about the z_{loc} direction

$[N]$ = twist shape functions collected into a row matrix

$N_m(\zeta)$ = set of twist shape functions that are zero at the beam ends

q = distributed load on girder (positive downward)

q_{LRB} = exact lateral-roll buckling load

$q_{LRB,0}$ = classical lateral-roll buckling load derived by Mast

$\hat{q}_{LTB,0}$ = modal approximation of classical lateral-roll-buckling load

$q_{LRB,v}$ = lateral-roll buckling load of a girder with major-axis deflections due to gravity

$q_{LRB,vp}$ = lateral-roll buckling load of a girder with major-axis deflections due to gravity and prestressing

$q_{LRB,vpa}$ = lateral-roll buckling load of a girder with asymmetric overhangs and major-axis deflections due to gravity and prestressing

q_{LTB} = exact lateral-torsional buckling load

$q_{LTB,0}$ = classical lateral-torsional buckling load derived by Timoshenko and Gere

$\widehat{q}_{LTB,0}$ = modal approximation of classical lateral-torsional buckling load

$q_{LTB,v}$ = lateral-torsional buckling load of an end-supported girder with major-axis deflections due to gravity

$q_{LTB,vp}$ = lateral-torsional buckling load of an end-supported girder with major-axis deflections due to gravity and prestressing

$q_{LTB,vp\alpha}$ = lateral-torsional buckling load of a girder with asymmetric overhangs and major-axis deflections due to gravity and prestressing

q_{LTRB} = near-exact lateral-torsional-roll buckling load, from the near-exact interaction equation solution form

$q_{LTRB,0}$ = basic lateral-torsional-roll buckling load for an end-supported girder with no major-axis deflections

$\hat{q}_{LTRB,0}$ = one-mode approximate lateral-torsional-roll buckling line load of a girder without major-axis deflection, prestressing or overhangs

$q_{LTRB,vp}$ = lateral-torsional-roll buckling load of a girder with major-axis deflections due to gravity and prestressing

$q_{LTRB,vp\alpha}$ = lateral-torsional-roll buckling load of a girder with asymmetric overhangs and major-axis deflections due to gravity and prestressing

q_p = nominal prestressing load, idealized as uniformly distributed load (typically upward, and therefore negative)

q_{sw} = uniformly distributed girder self-weight

r_{yy} = minor-axis radius of gyration

R = shear reaction at girder support (positive downward)

$s_j(t)$ = fourth-order polynomial in t, representing the effects of asymmetric overhangs

t = girder's level of asymmetry, as a function of the two end-overhang lengths

T = external restoring torque

u_{glo} = x displacement component in the global reference frame

u_{loc} = x displacement components in the local reference frame

$\overline{u}_{loc}$ = center-of-mass displacement in x_{loc} direction of a torsionally rigid, end-supported girder subjected to a uniform distributed line load in the absence of camber

v_{glo} = y displacement components in the global reference frame

v_{loc} = y displacement components in the local reference frame

$v_{loc,p}$ = displacement in y_{loc} direction due to prestress (that is, uplift)

$\overline{v}_{loc,p}$ = center-of-mass displacement in y_{loc} direction of a torsionally rigid, end-supported girder with prestressing load

$\overline{v}_{loc,v}$ = center-of-mass displacement in yloc direction of a torsionally rigid, end-supported girder subject to uniform distributed line load

$\overline{v}_{loc,vp}$ = center-of-mass displacement in yloc direction of a torsionally rigid, end-supported girder due to gravity and prestressing

w_c = concrete density

w_{glo} = z displacement components in the global reference frame

w_{loc} = z displacement components in the local reference frame

W = total girder weight

x_{glo} = x position coordinate in the global reference frame

x_{loc} = x position coordinate in the local reference frame

y_{glo} = y position coordinate in the global reference frame

y_{loc} = y position coordinate in the local reference frame

y_r = vertical (hanging) distance from the center of gravity of concrete to the support point

$y_{r,eff}$ = effective hanging distance for asymmetrically supported, torsionally rigid girder with different equivalent hanging distances at each support

$y_{r,eq}$ = equivalent hanging distance (valid for a hanging girder or a girder supported from below)

$y_{r1,eq}$ = equivalent hanging distance at support 1

$y_{r2,eq}$ = equivalent hanging distance at support 2

z = measure of distance along girder length

z_{glo} = z position coordinate in the global reference frame

z_{loc} = z position coordinate in the local reference frame

α = ratio of overhang distance to total girder length (that is, overhang ratio)

α_1 = overhang ratio at end 1

α_2 = overhang ratio at end 2

α_m = mean overhang ratio

β = dimensionless cross-sectional parameter

Δ = displacement of a prismatic simply supported beam subject to a distributed load

κ = load parameter = $q\sqrt{GJEI_{yy}}$

η_0 = torsion parameter of an end-supported girder with rigid major axis

η_{vp} = torsion parameter of an end-supported girder with major-axis deflections due to gravity and prestressing

$\eta_{vp\alpha}$ = torsion parameter of a girder with asymmetric overhangs and major-axis deflections due to gravity and prestressing

υ = Poisson's ratio

θ = rotation about longitudinal z axis

θ_i = initial girder roll angle due to eccentric lifting-loop support

θ_0 = rigid-body roll at supports

$\theta(0)$ = rotation angle at end 1, equal to the rigid-body roll θ_0 if girder is symmetric

$\theta(1)$ = rotation angle at end 2, equal to the rigid-body roll θ_0 if girder is symmetric

$\bar{\theta}(\zeta)$ = approximation of the beam twist along the length

$\hat{\theta}(\zeta)$ = weight function in the weak form of the twist-governing equation

ζ = normalized measure of distance along girder length [0,1]

About the authors

William D. Galik is a Ph.D candidate in the ROSE School of Earthquake Engineering within the University School for Advanced Studies at Scuola Universitaria Superiore Pavia (IUSS) in Pavia, Italy.

Richard Wiebe is an associate professor of civil and environmental engineering at the University of Washington in Seattle.

John F. Stanton is a professor of civil and environmental engineering at the University of Washington.

Abstract

Lateral buckling of precast and prestressed concrete girders that are not fully restrained against twisting rotations at their ends may occur during lifting and handling. Typically, the critical load at which this instability occurs has been estimated by ignoring torsional deformations. Although that approach permits a closed-formed solution, it is unconservative. This study includes the torsional deformations and develops a series solution for the simplest case of an end-supported girder. The solution is then extended to include overhangs. A balance between accuracy and usability is struck by truncating to a one-mode solution. By comparing with two known special cases, the first term is found to be sufficiently accurate while clearly illustrating the effect of torsional flexibility on girder stability.

Accounting for torsional deformations reduces the predicted buckling load by an amount that can be conveniently defined with a knockdown factor applied to the traditional buckling load that ignores torsion. In this sense, the effect of torsion is separated from lateral bending. Downward (major-axis) deflection improves stability, whereas that net upward camber does the opposite. Use of lightweight concrete reduces the safety factor against lateral buckling.

Keywords

Instability, prestressed concrete girder, roll buckling, torsion.

Review policy

This paper was reviewed in accordance with the Precast/Prestressed Concrete Institute's peer-review process. The Precast/Prestressed Concrete Institute is not responsible for statements made by authors of papers in *PCI Journal*. No payment is offered.

Publishing details

This paper appears in *PCI Journal* (ISSN 0887-9672) V. 69, No. 3, May–June 2024, and can be found at https://doi.org/10.15554/pcij69.3-01. *PCI Journal* is published bimonthly by the Precast/Prestressed Concrete Institute, 8770 W. Bryn Mawr Ave., Suite 1150, Chicago, IL 60631.

Reader comments

Please address any reader comments to *PCI Journal* editor-in-chief Tom Klemens at tklemens@pci.org or Precast/Prestressed Concrete Institute, c/o *PCI Journal*, 8770 W. Bryn Mawr Ave., Suite 1150, Chicago, IL 60631.

Appendix: Formulation of governing equation

Equation (29) governs the twist of girders under distributed loads in the major-axis plane. Multiple versions of this equation for special cases (for example, point loads and uniformly distributed loads) can be found in research articles and textbooks, such as Timoshenko and Gere.[1] Although not new, the formulation is included here to ensure a more self-contained description with a consistent sign convention and notation. Due to the assumptions used to develop the equation, it is limited to the prediction of the onset lateral-torsional buckling and lateral-torsional-roll buckling for girders with negligible major-axis deflection, no upwards prestressing deflection, and no overhangs. Various alternative sign conventions are used in the literature; however, the result seen in Eq. (29) is unchanged.

$$\frac{d^2\theta(\zeta)}{d\zeta^2}+\frac{\kappa^2 L^6}{4}\zeta^2(1-\zeta)^2\theta(\zeta)=0 \qquad (29)$$

where

θ = girder rotation about longitudinal z axis, along length

ζ = normalized measure of distance along girder length (0,1)

κ = load parameter = $q\sqrt{GJEI_{yy}}$

q = distributed load on girder (positive downward)

GJ = torsional rigidity

EI_{yy} = minor-axis flexural rigidity

L = total beam length

General formulation for small deformations

The main components of the governing equation are the global-to-local moment transformation; the net cross-section action relationships (kinematic and constitutive laws); and the moment-shear relationships (equilibrium). The moment transformation matrix for small angles can be obtained by reference to **Fig. A.1**, and is given by Eq. (A.1).

$$\begin{Bmatrix} M_{x,loc} \\ M_{y,loc} \\ M_{z,loc} \end{Bmatrix} = \begin{bmatrix} 1 & \theta & -u'_{glo} \\ -\theta & 1 & -v'_{glo} \\ u'_{glo} & v'_{glo} & 1 \end{bmatrix} \begin{Bmatrix} M_{x,glo} \\ M_{y,glo} \\ M_{z,glo} \end{Bmatrix} \qquad (A.1)$$

where

$M_{x,loc}$ = internal girder moment about the x_{loc} direction

x_{loc} = x position coordinate in the local reference frame

$M_{y,loc}$ = internal girder moment about the y_{loc} direction

y_{loc} = y position coordinate in the local reference frame

$M_{z,loc}$ = internal girder moment about the z_{loc} direction

z_{loc} = z position coordinate in the local reference frame

u'_{glo} = girder slope in the x_{glo}–z_{glo} plane

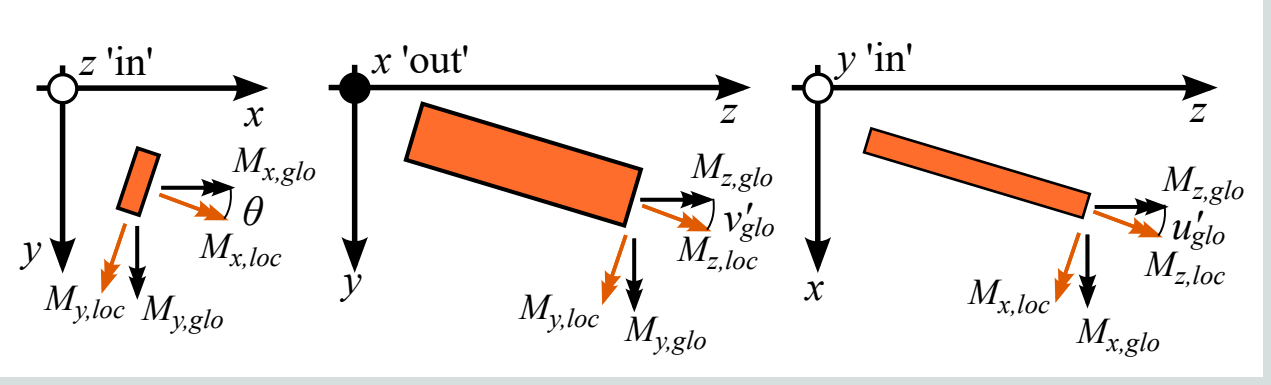

Figure A.1. Three perspectives of global and local moment sign convention displayed on a deformed girder segment. Note: $M_{x,glo}$ = internal beam moment in x_{glo} direction; $M_{x,loc}$ = internal beam moment in x_{loc} direction; $M_{y,glo}$ = internal beam moment in y_{glo} direction; $M_{y,loc}$ = internal beam moment in y_{loc} direction; $M_{z,glo}$ = internal beam moment in z_{glo} direction; $M_{z,loc}$ = internal beam moment in z_{loc} direction; u'_{glo} = girder slope in x_{glo}–z_{glo} plane; v'_{glo} = girder slope in y_{glo}-y_{glo} plane; z_{loc} = z position coordinates in the local reference frame; θ = girder twist about longitudinal z axis.

x_{glo} = x position coordinate in the global reference frame

z_{glo} = z position coordinate in the global reference frame

v'_{glo} = girder slope in the y_{glo}–z_{glo} plane

y_{glo} = y position coordinate in the global reference frame

$M_{x,glo}$ = internal girder moment about the x_{glo} direction

$M_{y,glo}$ = internal girder moment about the y_{glo} direction

$M_{z,glo}$ = internal girder moment about the z_{glo} direction

The global and local subscripts are consistent with the approach for deformations in Fig. 4.

The benefit of having the moments written in the local cross-section axes is the direct application of the well-known net cross-section action-deformation relationships given by Eq. (A.2).

$$\begin{Bmatrix} M_{x,loc} \\ M_{y,loc} \\ M_{z,loc} \end{Bmatrix} = \begin{Bmatrix} -EI_{xx}v''_{loc} \\ EI_{yy}u''_{loc} \\ GJ\theta' \end{Bmatrix} \approx \begin{Bmatrix} -EI_{xx}v''_{glo} \\ EI_{yy}u''_{glo} \\ GJ\theta' \end{Bmatrix} \quad \text{(A.2)}$$

EI_{xx} = major-axis flexural rigidity

u''_{glo} = girder curvature in the x_{glo}–z_{glo} plane

u''_{loc} = girder curvature in the x_{loc}–z_{loc} plane

v''_{glo} = girder curvature in the y_{glo}–z_{glo} plane

v''_{loc} = girder curvature in the y_{loc}–z_{loc} plane

θ' = girder twist gradient

The negative sign in the $M_{x,loc}$ expression is a consequence of the sign convention chosen in Fig. A.1. The torsion component here assumes St. Venant torsion behavior, which is reasonable as warping restraint is insignificant in hanging girders. The approximation of local curvatures by global values limits the suitability of the resulting equation for predicting the onset of buckling (not postbuckling behavior) with negligible prebuckling deformation in the loaded major axis. In addition, the local and global twist gradients not identical in the large deformation sense, though the global quantity θ' is assumed to be representative of the local quantity.

Equating the two $M_{y,loc}$ expressions in Eq. (A.1) and (A.2) yields the relationship in Eq. (A.3), which will be used to arrive at the final result.

$$EI_{yy}u''_{glo} = -\theta M_{x,glo} + M_{y,glo} - v'_{glo}M_{y,glo} \quad \text{(A.3)}$$

The moment equilibrium equations can be obtained from the free-body diagram in **Fig. A.2**. The distributed loads are not shown; however, they appear as higher-order terms in the moment equilibrium expressions. Applying moment equilibrium results in Eq. (A.4) to Eq. (A.6).

$$M'_{x,glo} = V_{y,glo} \quad \text{(A.4)}$$

where

$M'_{x,glo}$ = differentiation of $M_{x,glo}$ by the global longitudinal coordinate z_{glo}

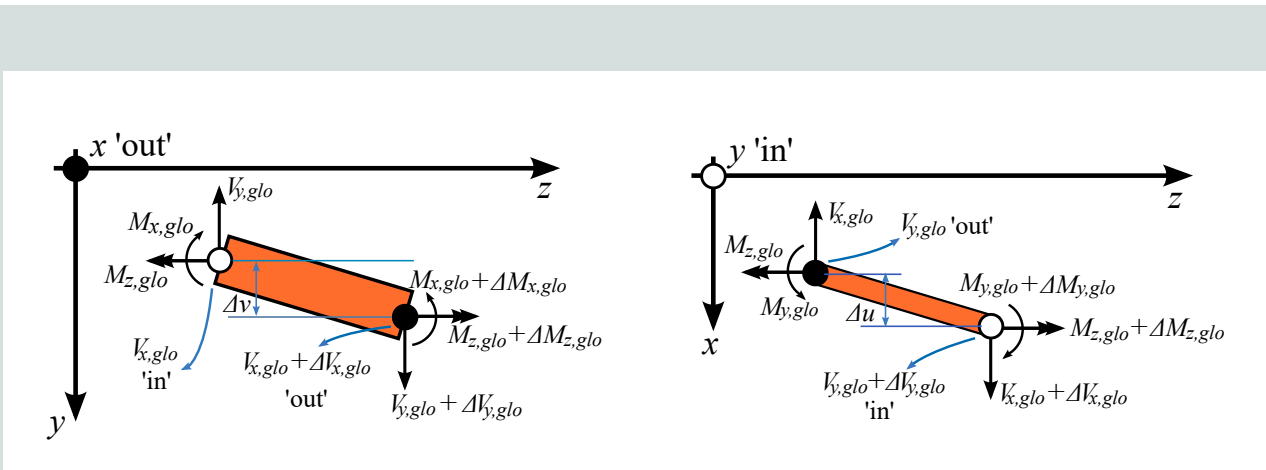

Figure A.2. Two perspectives of free-body diagram of a deformed girder segment. Note: distributed loads are not shown for brevity. $M_{x,glo}$ = internal beam moment in x_{glo} direction; $M_{y,glo}$ = internal beam moment in y_{glo} direction; $M_{z,glo}$ = internal beam moment in z_{glo} direction; $V_{x,glo}$ = internal beam shear in x_{glo} direction; $V_{y,glo}$ = internal beam shear in y_{glo} direction; $\Delta M_{x,glo}$ = change in internal beam moment in x_{glo} direction, along differential element; $\Delta M_{y,glo}$ = change in internal beam moment in y_{glo} direction, along differential element; $\Delta M_{z,glo}$ = change in internal beam moment in z_{glo} direction, along differential element; Δu_{glo} = change in x_{glo} displacement along differential element; Δv_{glo} = change in y_{glo} displacement along differential element; $\Delta V_{x,glo}$ = change in $V_{x,glo}$ along differential element; $\Delta V_{y,glo}$ = change in $V_{y,glo}$ along differential element.

z_{glo} = measure of distance along girder length

$V_{y,glo}$ = internal girder shear in y_{glo} direction

$$M'_{y,glo} = -V_{x,glo} \tag{A.5}$$

where

$V_{x,glo}$ = internal girder shear in x_{glo} direction

$$M'_{z,glo} = V_{x,glo}v'_{glo} - V_{y,glo}u'_{glo} \tag{A.6}$$

where

$M'_{z,glo}$ = differentiation of $M_{z,glo}$ by the global longitudinal coordinate z_{glo}

Eliminating the local moments from the left-hand side of Eq. (A.1) using Eq. (A.2), and differentiating both sides (including the product rule on the right-hand side) yields Eq. (A.7).

$$\begin{Bmatrix} -EI_{xx}v'''_{glo} \\ EI_{yy}u'''_{glo} \\ GJ\theta'' \end{Bmatrix} = \begin{bmatrix} 0 & \theta' & -u''_{glo} \\ -\theta' & 0 & -v''_{glo} \\ u''_{glo} & v''_{glo} & 1 \end{bmatrix} \begin{Bmatrix} M_{x,glo} \\ M_{y,glo} \\ M_{z,glo} \end{Bmatrix} + \begin{bmatrix} 1 & \theta & -u'_{glo} \\ -\theta & 1 & -v'_{glo} \\ u'_{glo} & v'_{glo} & 1 \end{bmatrix} \begin{Bmatrix} M'_{x,glo} \\ M'_{y,glo} \\ M'_{z,glo} \end{Bmatrix} \tag{A.7}$$

where

v'''_{glo} = rate of change of beam curvature in y_{glo}–z_{glo} plane

u'''_{glo} = rate of change of beam curvature in x_{glo}–z_{glo} plane

θ'' = girder twist curvature

Thereafter applying Eq. (A.4) through Eq. (A.6) to eliminate the moment gradients on the right-hand side, and neglecting higher-order terms (small-deformation assumption) gives Eq. (A.8), for which several terms cancel out in the third expression.

$$\begin{Bmatrix} -EI_{xx}v'''_{glo} \\ EI_{yy}u'''_{glo} \\ GJ\theta'' \end{Bmatrix} = \begin{bmatrix} 0 & \theta' & -u''_{glo} \\ -\theta' & 0 & -v''_{glo} \\ u''_{glo} & v''_{glo} & 1 \end{bmatrix} \begin{Bmatrix} M_{x,glo} \\ M_{y,glo} \\ M_{z,glo} \end{Bmatrix} + \begin{Bmatrix} V_{y,glo} - \theta V_{x,glo} \\ -\theta V_{y,glo} - V_{x,glo} \\ 0 \end{Bmatrix} \tag{A.8}$$

where

$V_{x,glo}$ = girder internal shear in the x_{glo} direction

Special case: global major-axis moment only

The scenario of interest in this work, and in many other applications, is beams and girders predominantly loaded in their major axis. In this case, $M_{y,glo}$ equals $M_{z,glo}$ equals 0 and V_x equals 0. The governing equations therefore simplify to Eq. (A.9).

$$\begin{Bmatrix} -EI_{xx}v'''_{glo} \\ EI_{yy}u'''_{glo} \\ GJ\theta'' \end{Bmatrix} = \begin{Bmatrix} V_{y,glo} \\ -\theta' M_{x,glo} - \theta V_{y,glo} \\ u''_{glo} M_{x,glo} \end{Bmatrix} \tag{A.9}$$

The first, uncoupled, equation governs the major-axis bending. The latter two describe the interaction between lateral deformation and twist. Finally, Eq. (A3) (again with $M_{y,glo}$ equals $M_{z,glo}$ equals 0) can be used to eliminate u''_{glo} from the twist expression, giving Eq. (10), the final equation governing the girder rotation (letting z_{glo} equal the distance along girder length z, for brevity).

$$\theta'' + \frac{M^2_{x,glo}(z)}{GJEI_{yy}}\theta = 0 \tag{A.10}$$

This equation is well known; however, it is often derived for the special case of a constant moment. Hence, it is less well known that this expression is general for any moment gradient. For a simply supported beam with distributed load q:

$$M_{x,glo}(z) = \frac{q}{2}(L - z)z$$

Making this substitution, along with the change of variables (ζ equals z/L) yields the expression in Eq. (29).

Reference

1. Timoshenko, S. P., and J. M. Gere. 1961. *Theory of Elastic Stability*. New York, NY: McGraw-Hill.

Notation

EI_{xx} = major-axis flexural rigidity

EI_{yy} = minor-axis flexural rigidity

GJ = torsional rigidity

L = total beam length

M = number of mode shapes included in the twist approximation

$M_{x,glo}$ = internal beam moment in x_{glo} direction

$M'_{x,glo}$ = differentiation of $M_{x,glo}$ by the global longitudinal coordinate z_{glo}

$M_{x,loc}$ = internal beam moment in x_{loc} direction

$M_{y,glo}$ = internal beam moment in y_{glo} direction

$M_{y,loc}$ = internal beam moment in y_{loc} direction

$M_{z,glo}$ = internal beam moment in z_{glo} direction

$M'_{z,glo}$ = differentiation of $M_{z,glo}$ by the global longitudinal coordinate z_{glo}

$M_{z,loc}$ = internal beam moment in z_{loc} direction

q = distributed load on girder (positive downward)

u'_{glo} = girder slope in the x_{glo}–z_{glo} plane

u''_{glo} = girder curvature in the x_{glo}–z_{glo} plane

u'''_{glo} = rate of change of beam curvature in x_{glo}–z_{glo} plane

u''_{loc} = girder curvature in the x_{loc}–z_{loc} plane

v'_{glo} = girder slope in the y_{glo}–z_{glo} plane

v''_{glo} = girder curvature in the y_{glo}–z_{glo} plane

v'''_{glo} = rate of change of beam curvature in y_{glo}–z_{glo} plane

v''_{loc} = girder curvature in the y_{loc}–z_{loc} plane

$V_{x,glo}$ = girder internal shear in the x_{glo} direction

$V_{y,glo}$ = girder internal shear in the y_{glo} direction

x_{glo} = x position coordinate in the global reference frame

x_{loc} = x position coordinate in the local reference frame

y_{glo} = y position coordinate in the global reference frame

y_{loc} = y position coordinate in the local reference frame

z = measure of distance along girder length

z_{glo} = z position coordinates in the global reference frame

z_{loc} = z position coordinate in the local reference frame

$\Delta M_{x,glo}$ = change in internal beam moment in x_{glo} direction, along differential element

$\Delta M_{y,glo}$ = change in internal beam moment in y_{glo} direction, along differential element

$\Delta M_{z,glo}$ = change in internal beam moment in z_{glo} direction, along differential element

Δu_{glo} = change in x_{glo} displacement along differential element

Δv_{glo} = change in y_{glo} displacement along differential element

$\Delta V_{x,glo}$ = change in $V_{x,glo}$ along differential element

$\Delta V_{y,glo}$ = change in $V_{y,glo}$ along differential element

θ = girder twist about longitudinal z_{glo} axis

θ' = girder twist gradient

θ'' = girder twist curvature

κ = load parameter = $q\sqrt{GJEI_{yy}}$

ζ = normalized measure of distance along girder length [0,1]